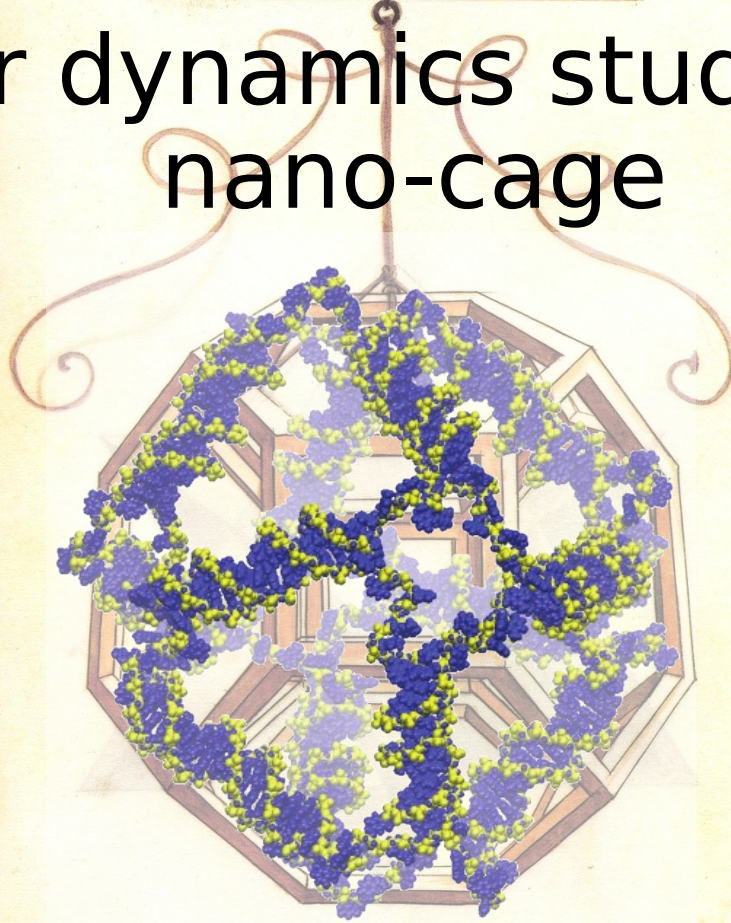


.C.

OCTOCEDRON ABSGISVS
VACVVS.

Molecular dynamics study of a DNA nano-cage

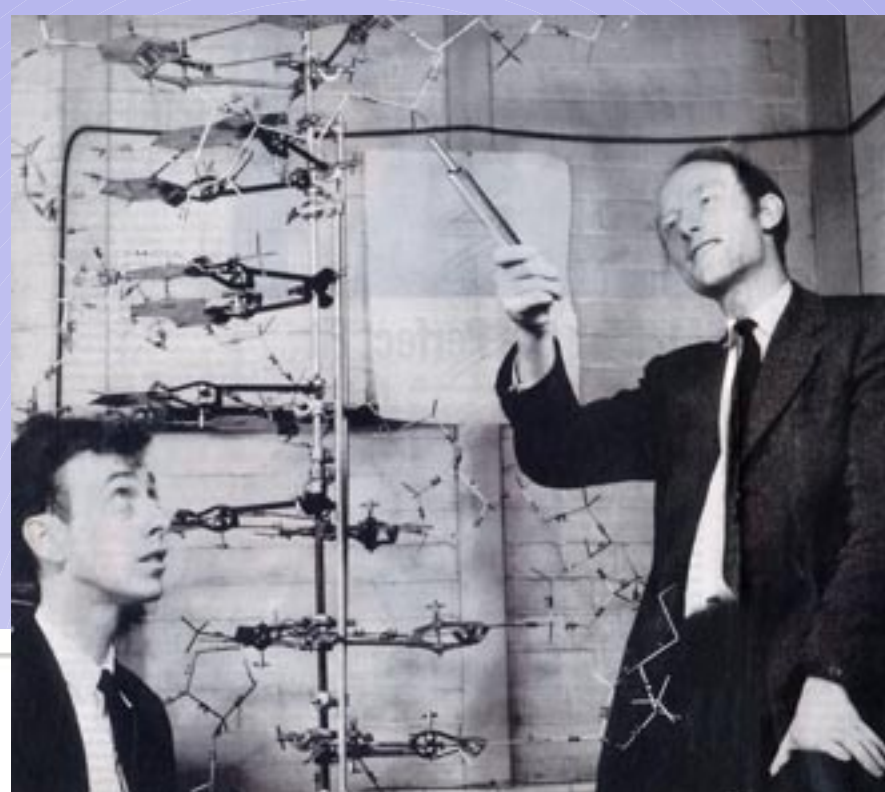


XVIII
11177

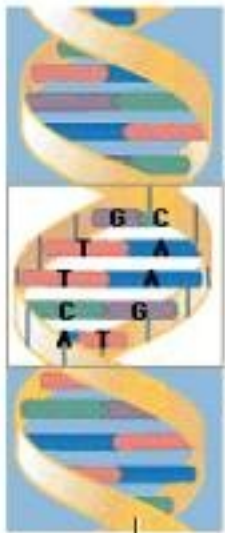
Οκταεδρον ἀβγισε δ' ἐν κενόν.

Alessandro Desideri
Università Roma Tor
Vergata

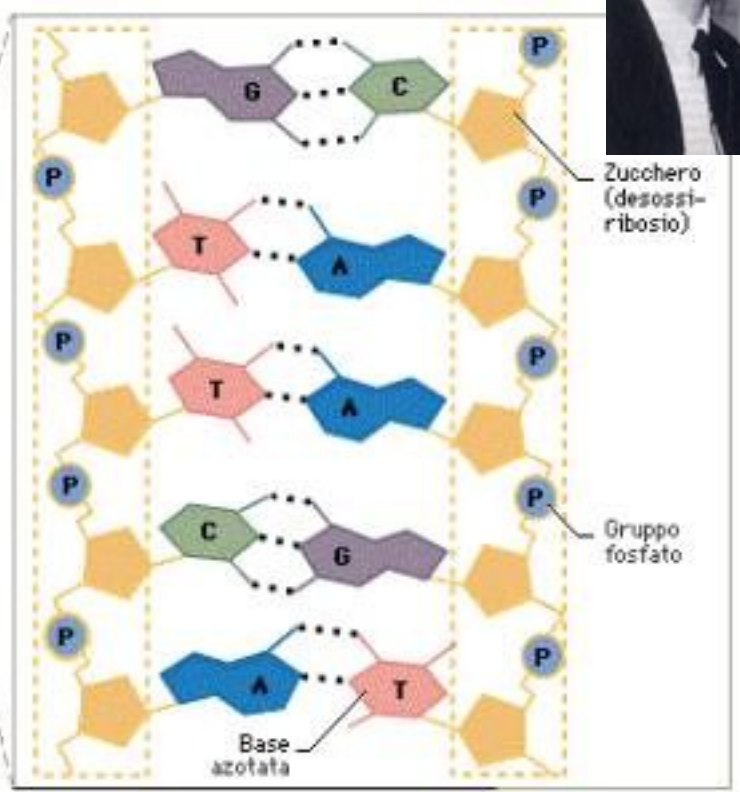
17/04/09



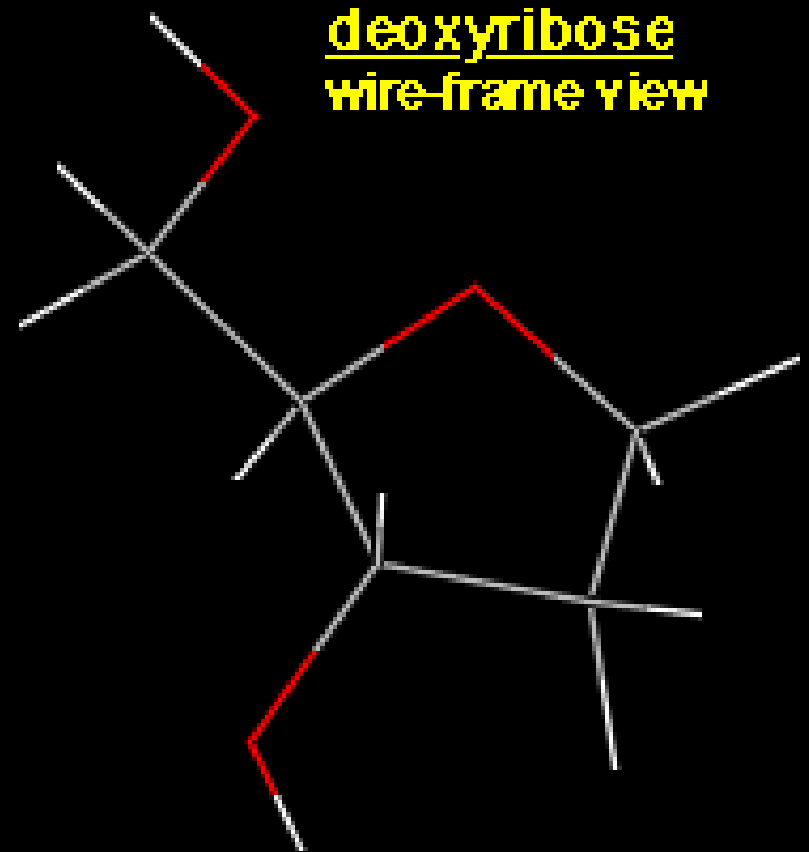
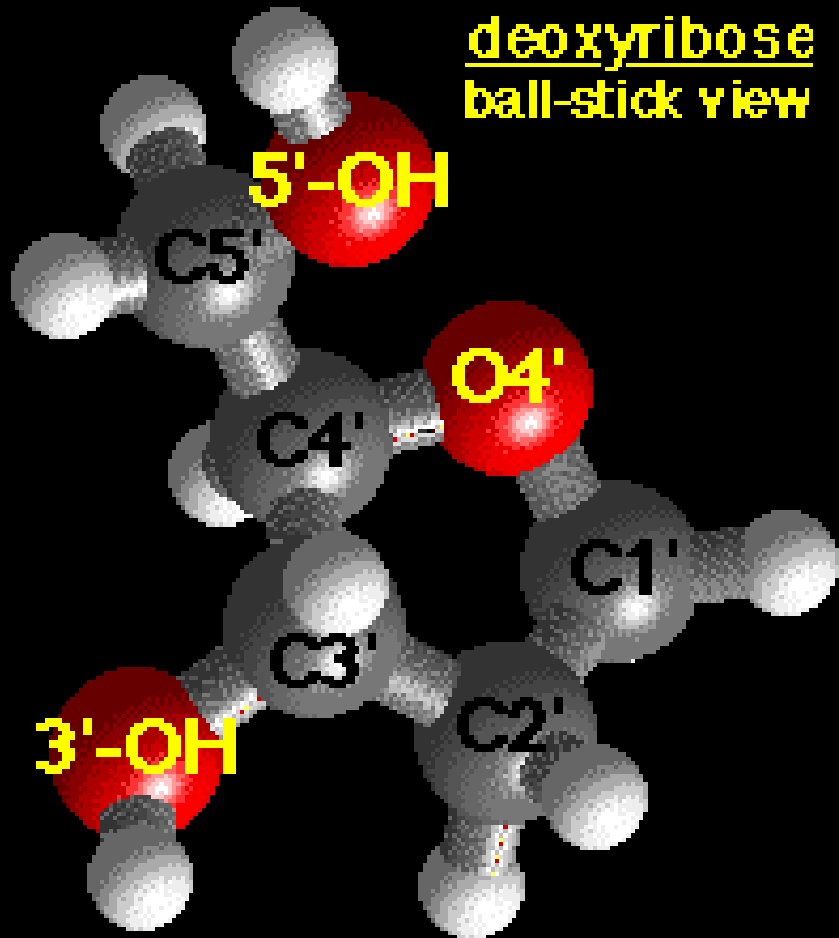
Modello a doppia elica del DNA



La struttura portante è costituita dalle molecole di zucchero alternate ai gruppi fosfato

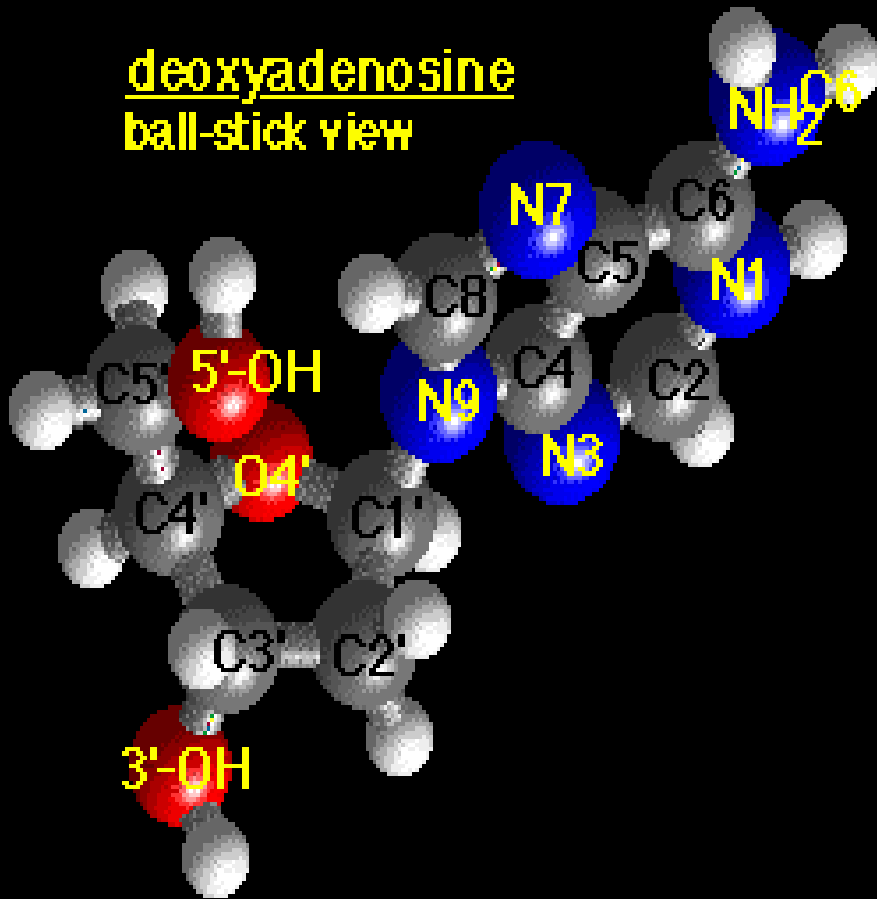


The deoxyribose sugar of the DNA backbone has 5 carbons and 3 oxygens. The carbon atoms are numbered 1', 2', 3', 4', and 5' to distinguish from the numbering of the atoms of the purine and pyrimidine rings. The hydroxyl groups on the 5'- and 3'- carbons link to the phosphate groups to form the DNA

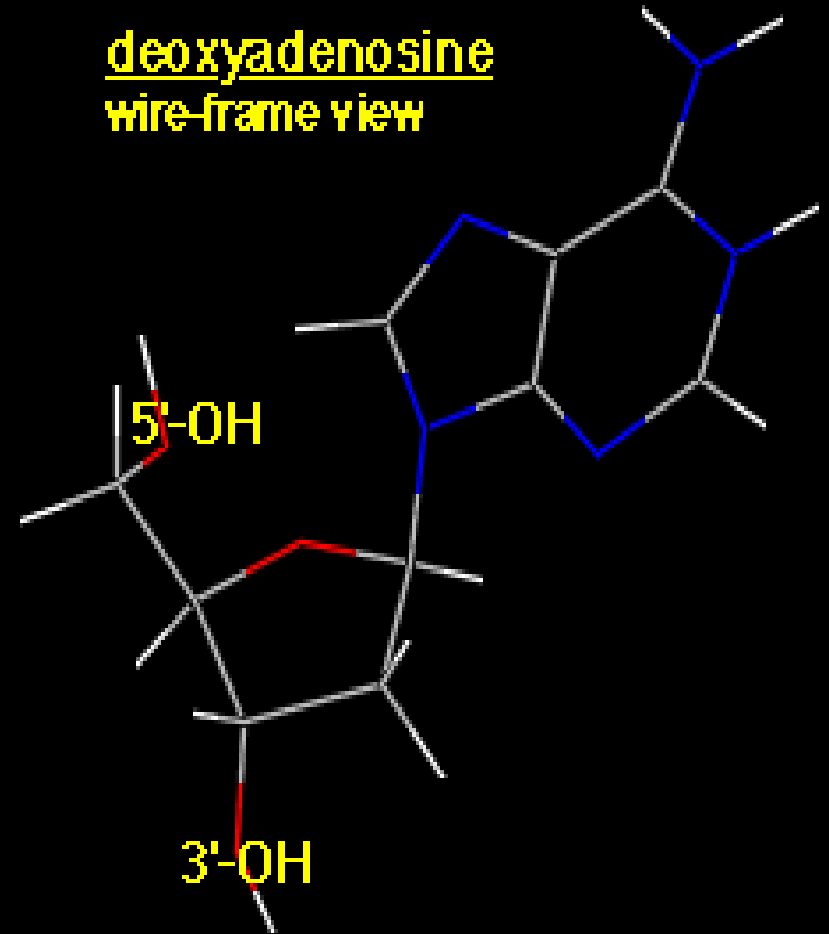


Nucleoside: base legata covalentemente al C1'

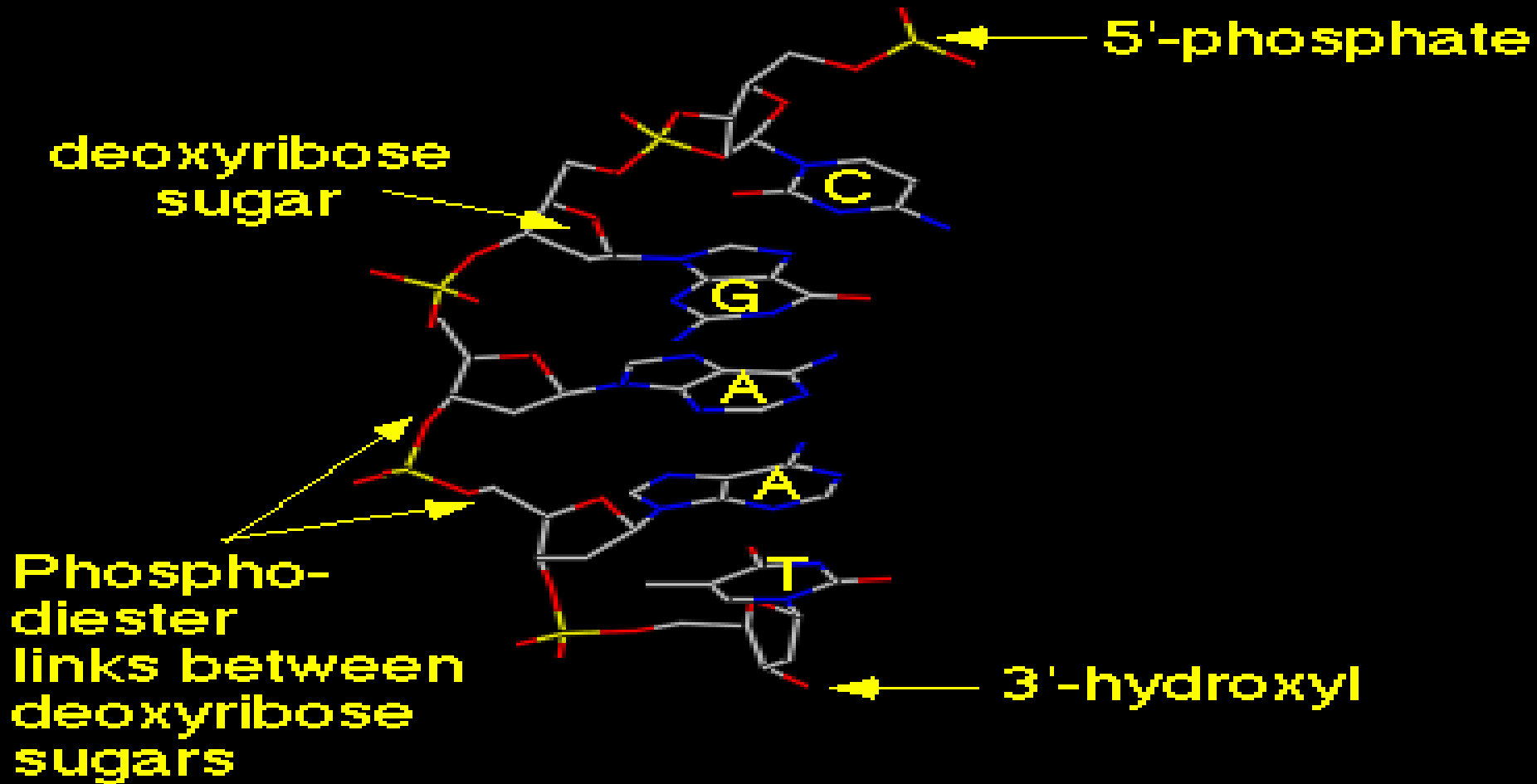
deoxyadenosine
ball-stick view



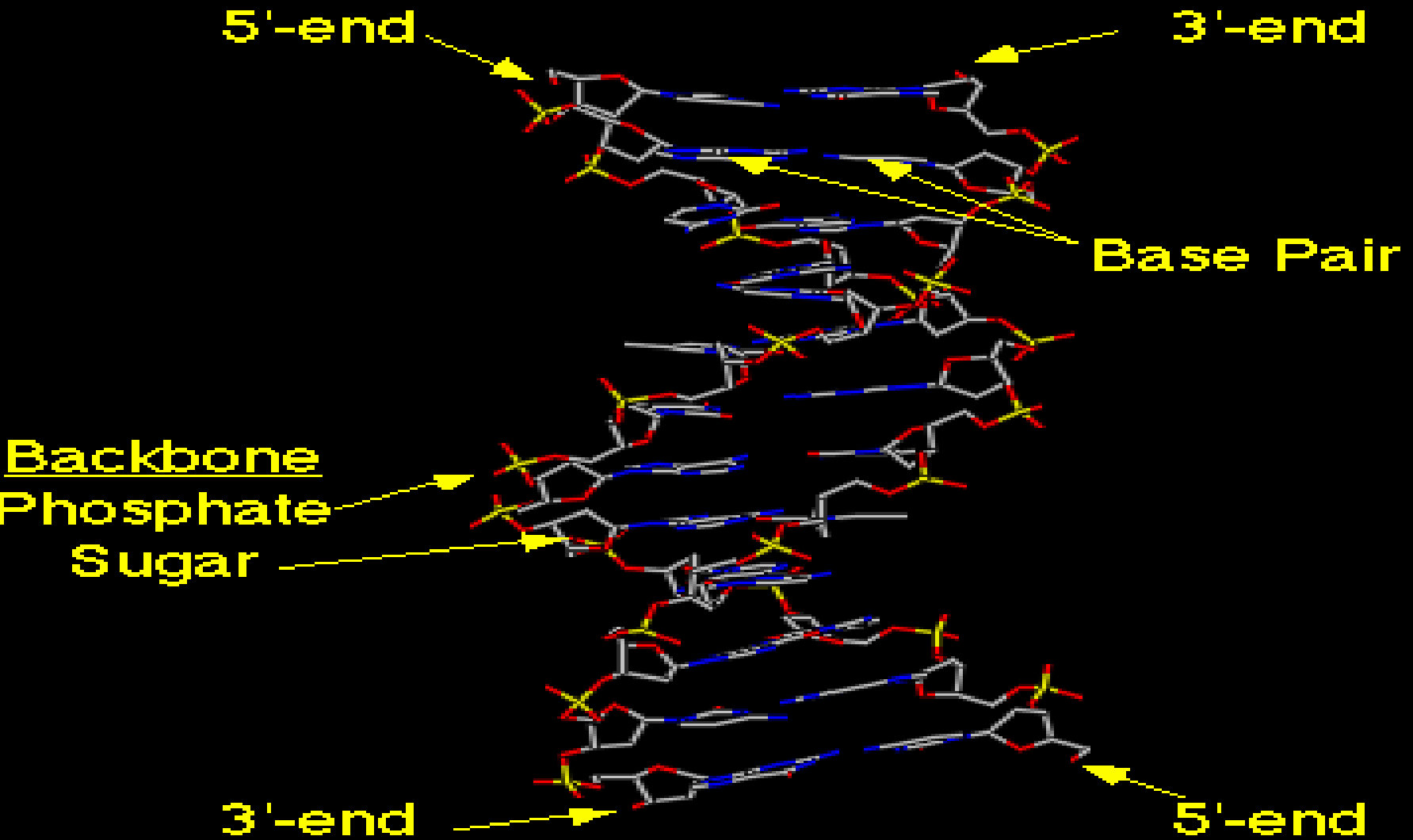
deoxyadenosine
wire-frame view



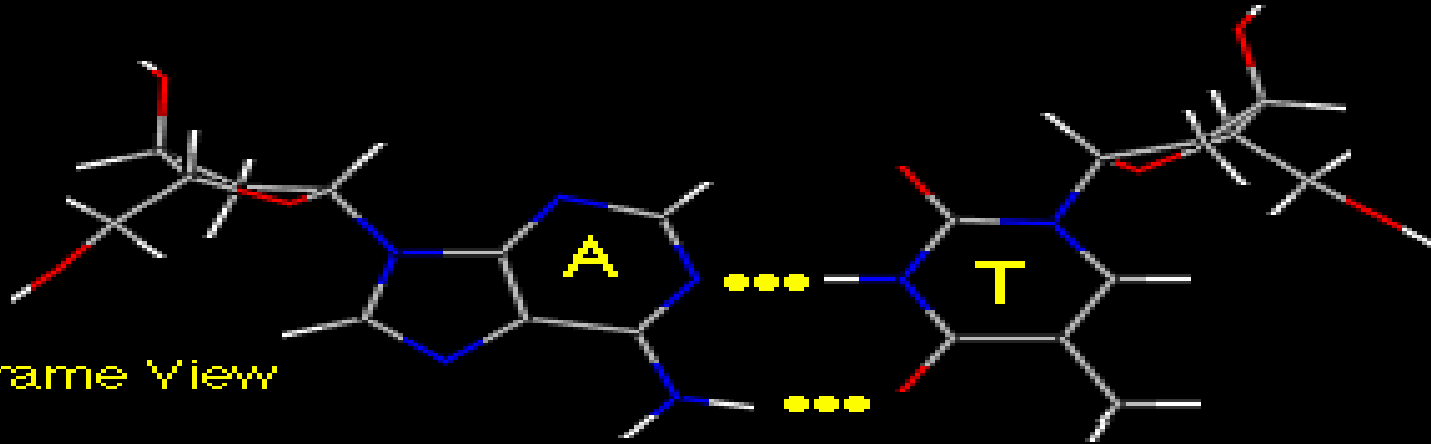
The deoxyribose sugars are joined at both the 3'-hydroxyl and 5'-hydroxyl groups to phosphate groups in ester links, also known as "phosphodiester" bonds.



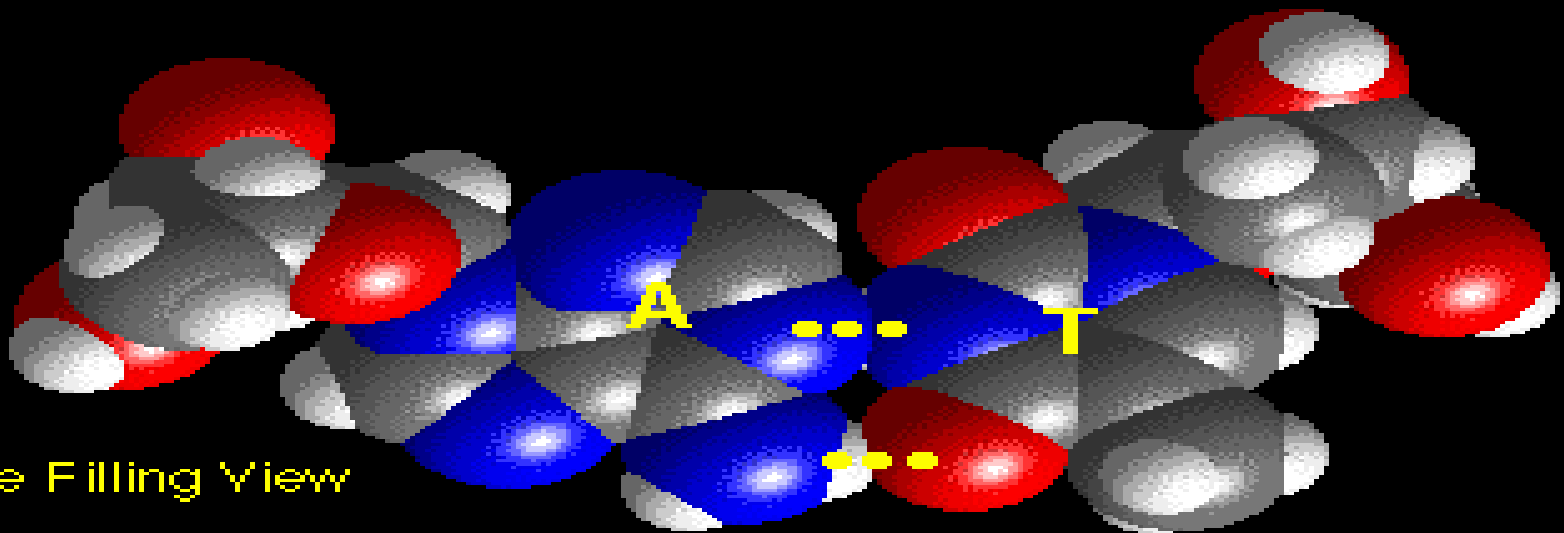
Doppio filamento



Legami idrogeno A·T

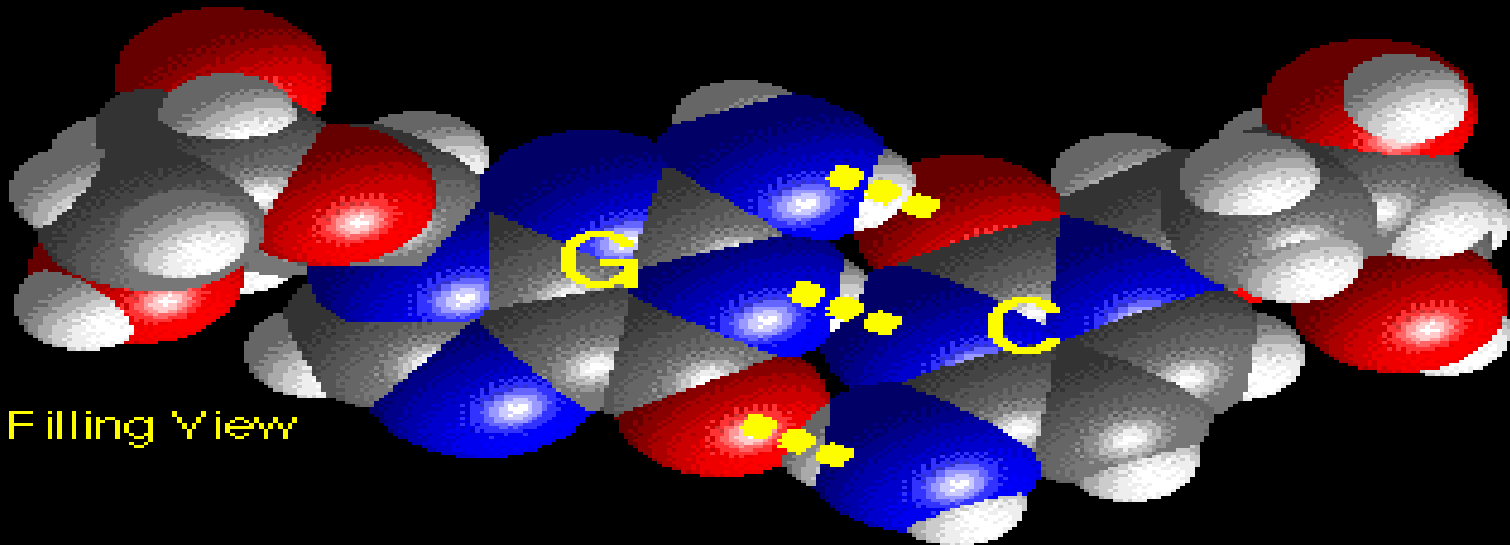
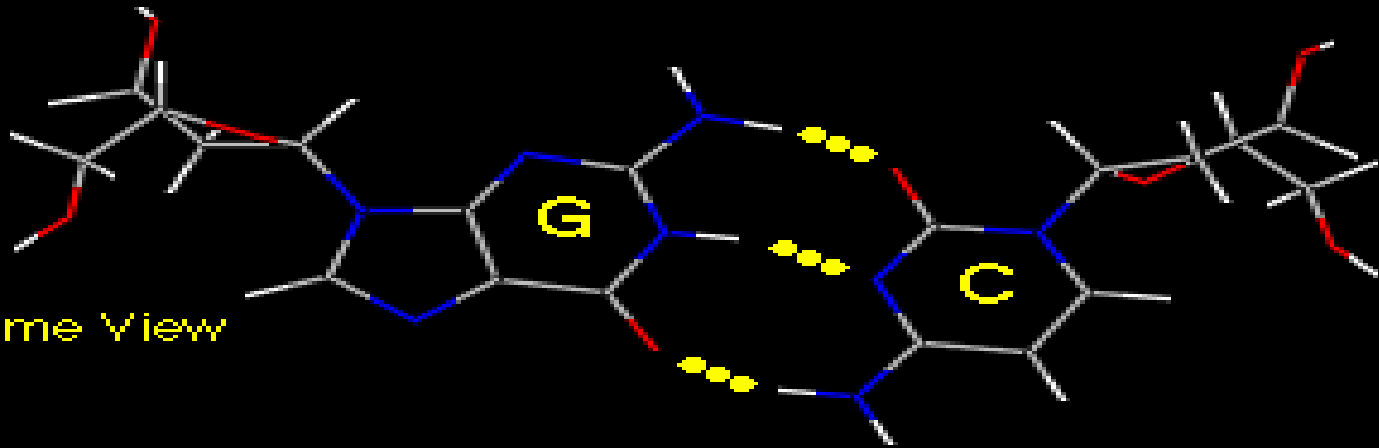


Wire Frame View



Space Filling View

Legami idrogeno G:C



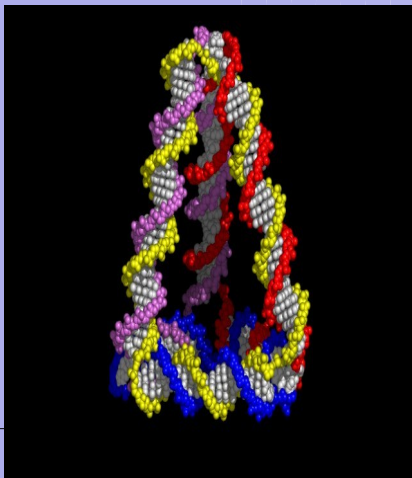
DNA nanostructure

DNA advantage:

- The code is composed by only four monomers and hence is easy to program
- The resulting structure is easily predictable

DNA nanostructure use:

- rigid building blocks
- molecular cages
- DNA motors and fuels
- application of DNA lattices to protein structure determination.

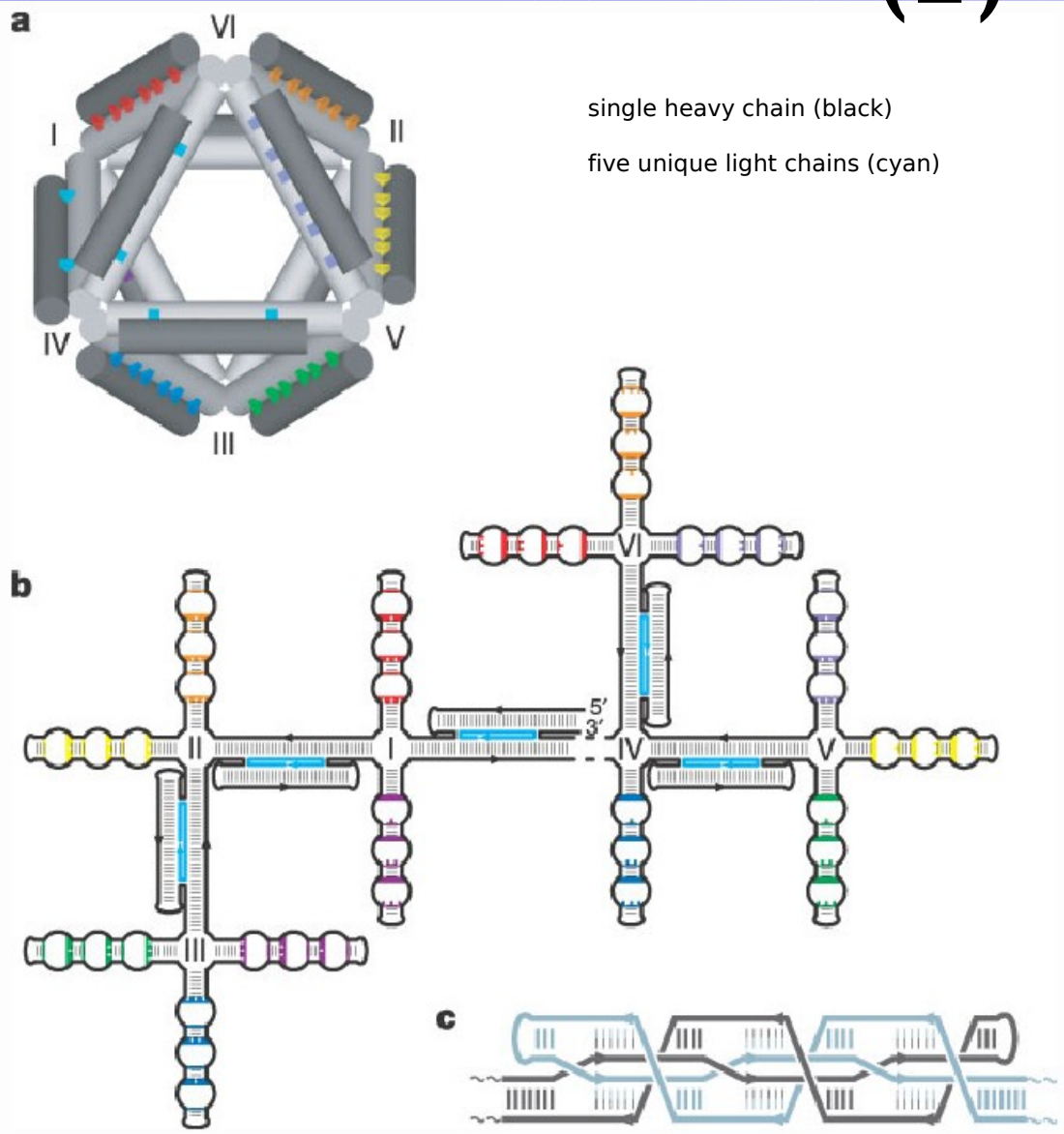


Reference:.

- Omabegho T., Sha R. Seeman NC A bipedal DNA Brownian Motor with coordinated legs, Science 2009 324 67-71
- R. P. Goodman, R. M. Berry, A. J. Turberfield, The single-step synthesis of a DNA tetrahedron, Chem. Comm. 1372-1373 (2004)
- J. Bath, S. J. Green, A. J. Turberfield, A free-running DNA motor powered by a nicking enzyme, Angew. Chem. Int. Ed. 44, 4358-4361 (2005)

NANOSCALE OCTAEDRONS

(2)



Folding was designed to occur in two stages

1) The heavy chain and the five light chains associate stoichiometrically and collapse into a branched-tree structure (Fig. 1b). Binding of the heavy and light chains forms double crossovers that provide five of the twelve struts of the target structure. This intermediate state has fourteen terminal branches, each corresponding to a half-strut. The terminal branches are unique 76-nucleotide loops, each with sequence complementarity (in the PX sense) to one and only one other loop sequence (Fig. 1c).

2) Conjugate terminal branches associate to form the remaining seven struts. The order of formation of the struts should not make a difference in achieving the final structure.

The DNA octahedron reported here contains no catenations or knots.

William M. Shih¹, Joel D. Quispe² & Gerald F. Joyce¹ A 1.7-kilobase single-stranded DNA that folds into a nanoscale octahedron. *Nature* (427), 2004.

Basic Requirement in DNA 3D Structure Design

- Maximizing the energy difference between the desired structure (lower energy) and the unwanted ones (higher energy)
- Linking the DNA ends covalently after assembly to prevent the structure disintegration
- Minimizing unwanted base pairing:
 - annealing between different oligonucleotides,
 - annealing between two identical oligonucleotides,
 - annealing within a single oligonucleotide

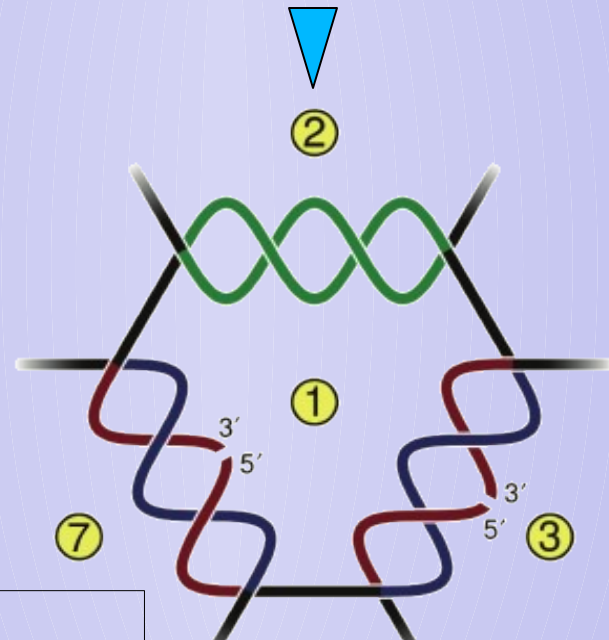
Design of oligonucleotides

- OL1
- OL2
- OL3
- OL4
- OL5
- OL6
- OL7
- OL8



Theoretical complementary green region annealing temperature = 56°C

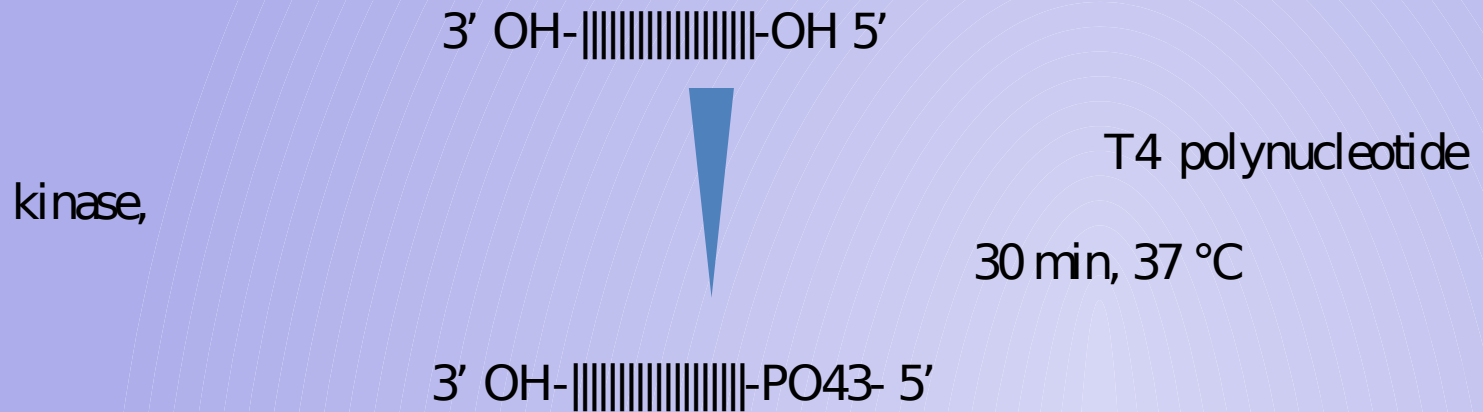
Theoretical complementary red-blue region annealing temperature = 28°C



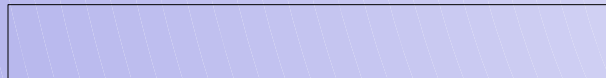
G1G2G3G4G5G6 G7G8 B1R3
 B7B4B9 R5 B4R2 B5R7 B6R4 B7R1
 B8R6

Assembling Procedure

- 5' extremities activation



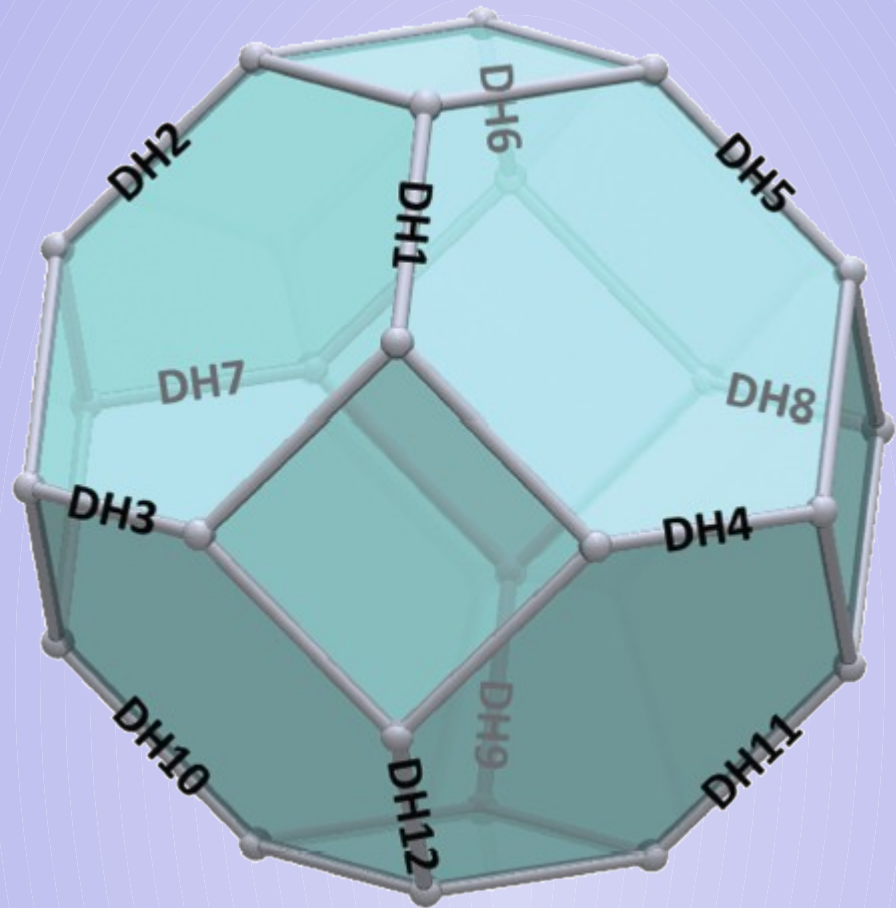
- Heating to 65°C for 10 min
- Cooling by 0.25°C/min until 30°C
- T4 DNA ligase addition
- Cooling by 0.25°C/min until 16°C



Predicted Structure

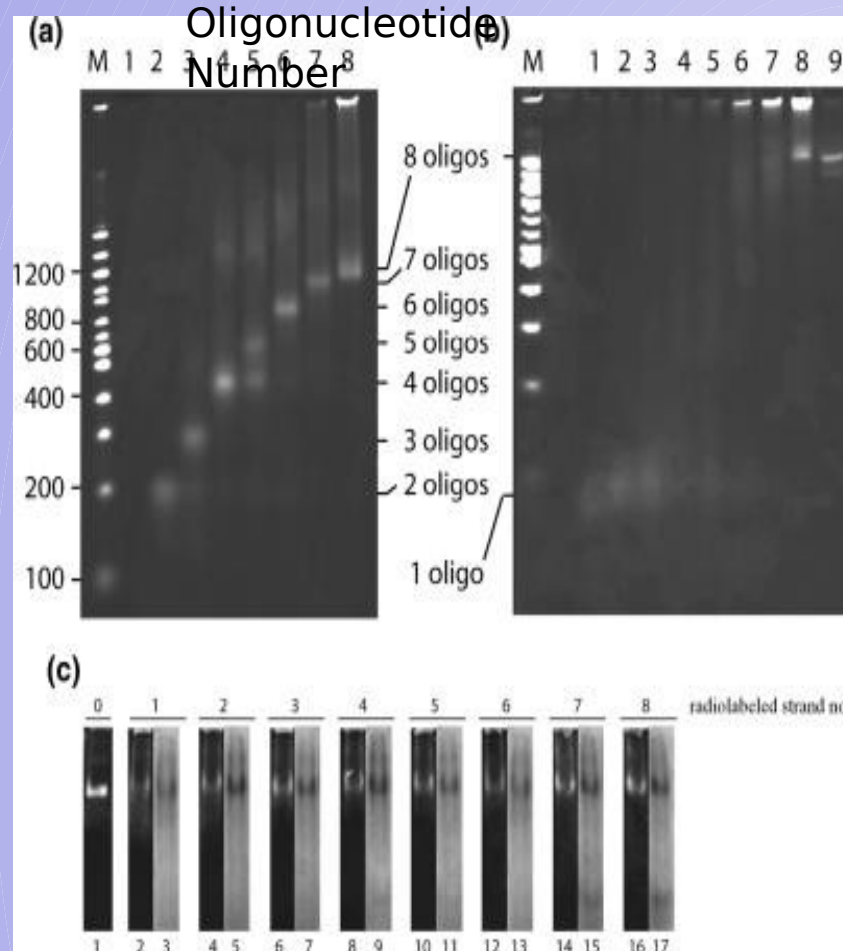
12 Double Helices

24 Seven Thymidine base-pair
Single Strand



17/04/09

Self-assembling specificity



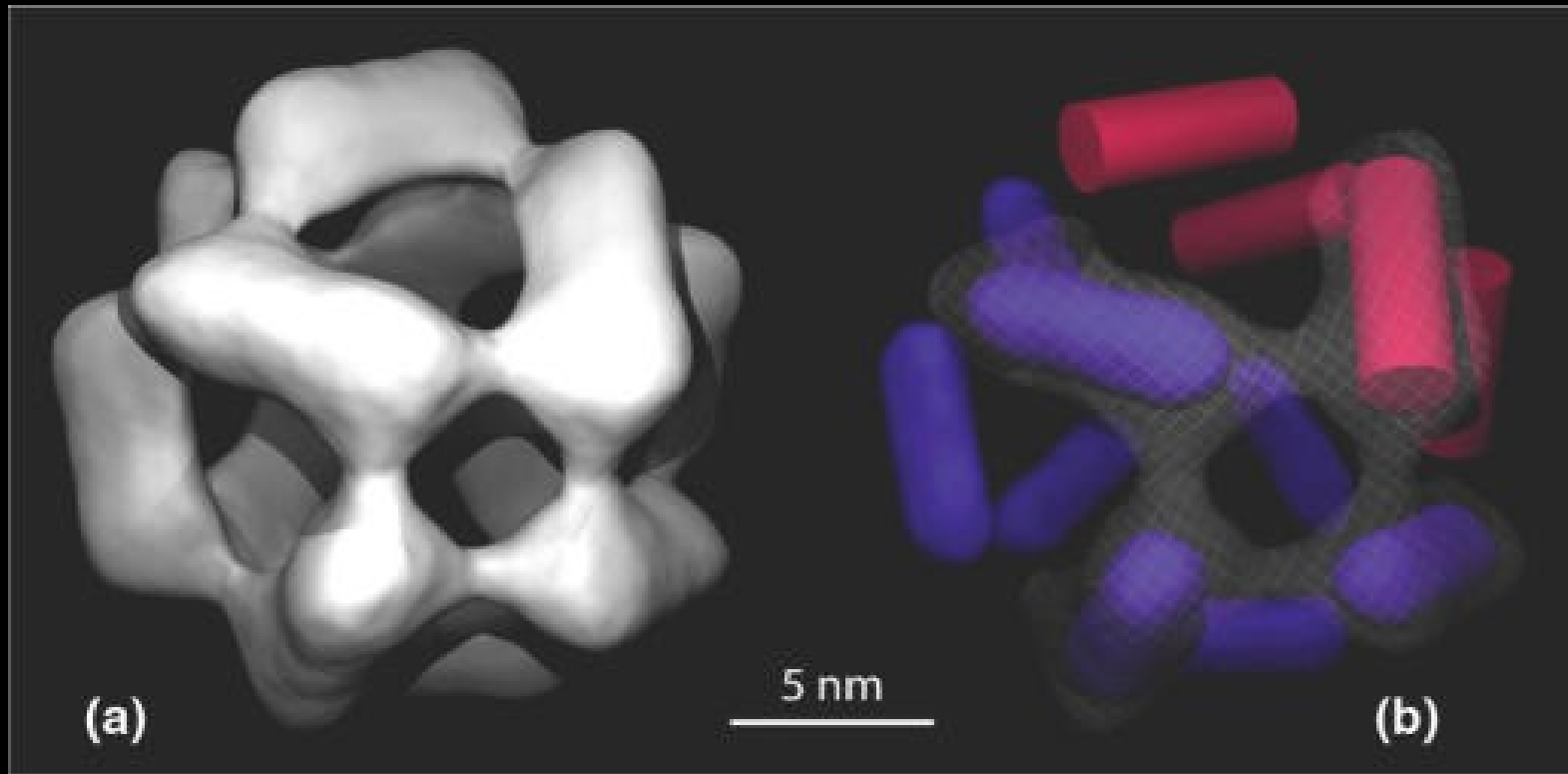
Andersen et. al. 2007

17/04/09

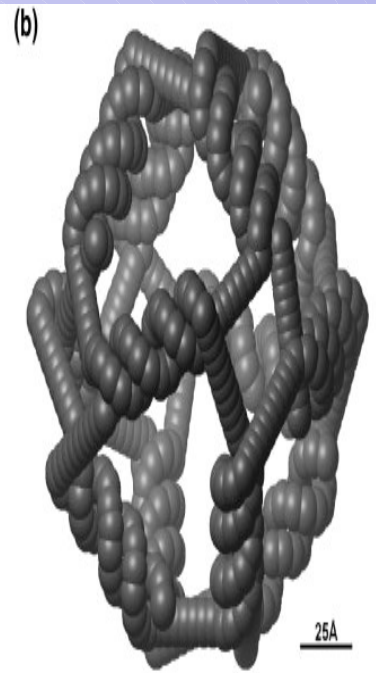
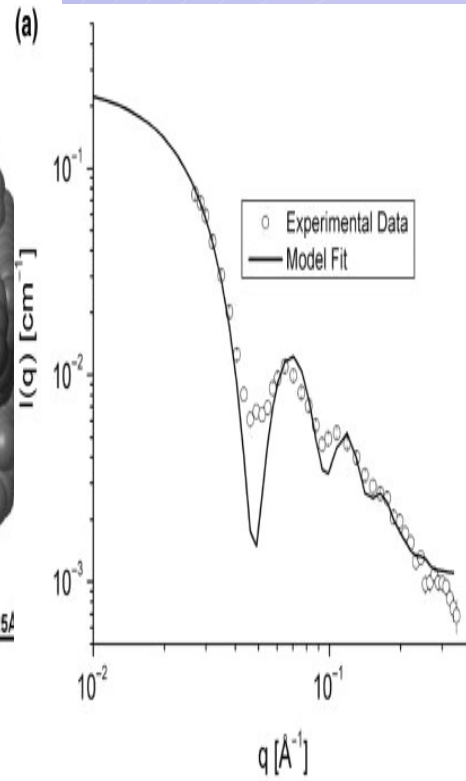
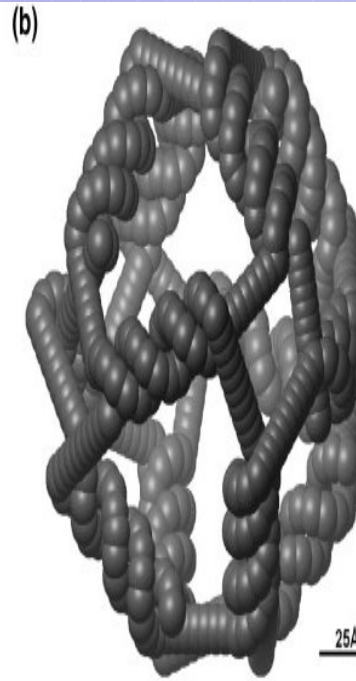
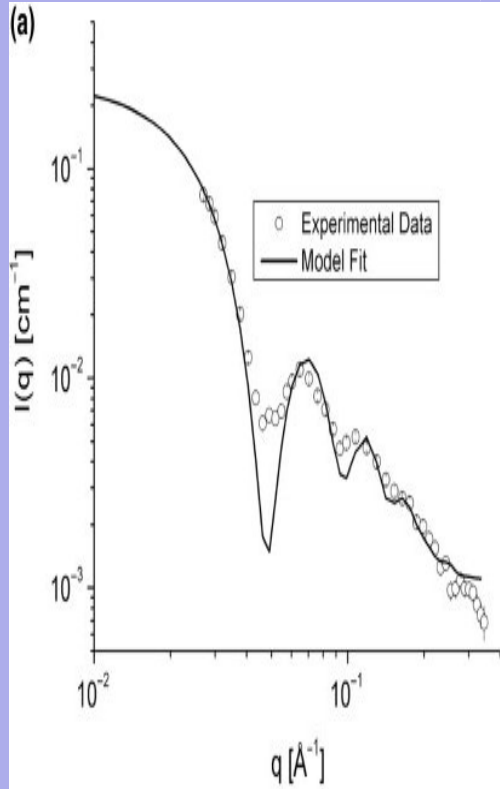
NATIVE

The Nanocage

cryo-TEM

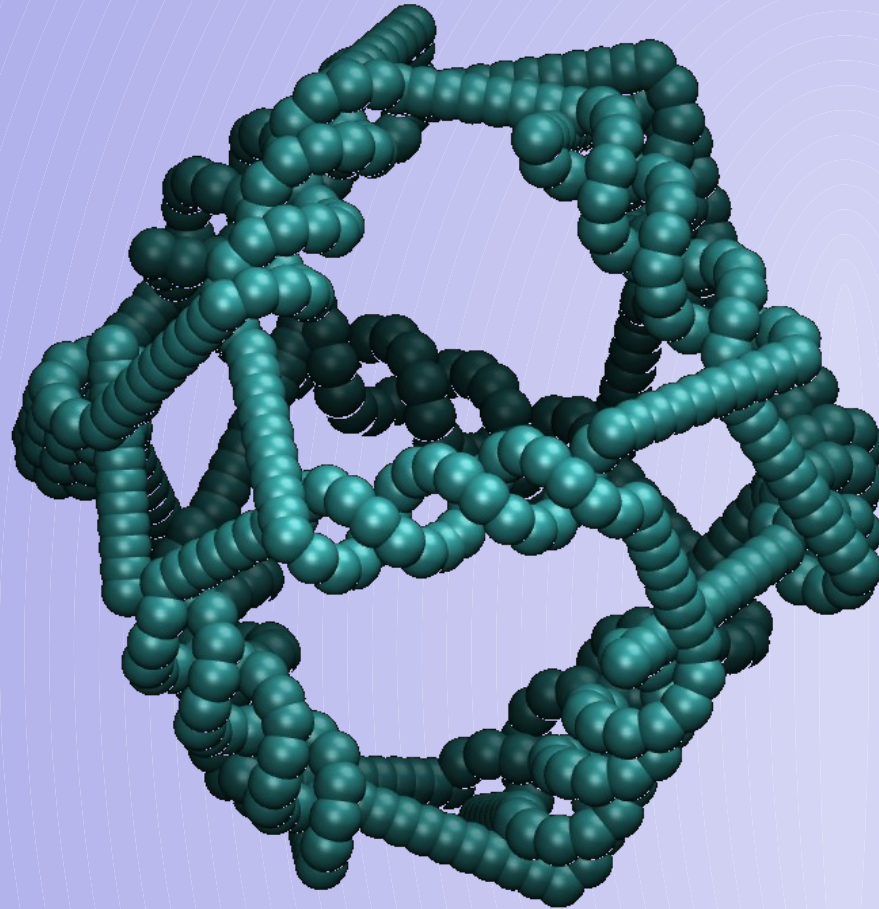


Andersen et. al.
2007



The Nanocage

Low Resolution



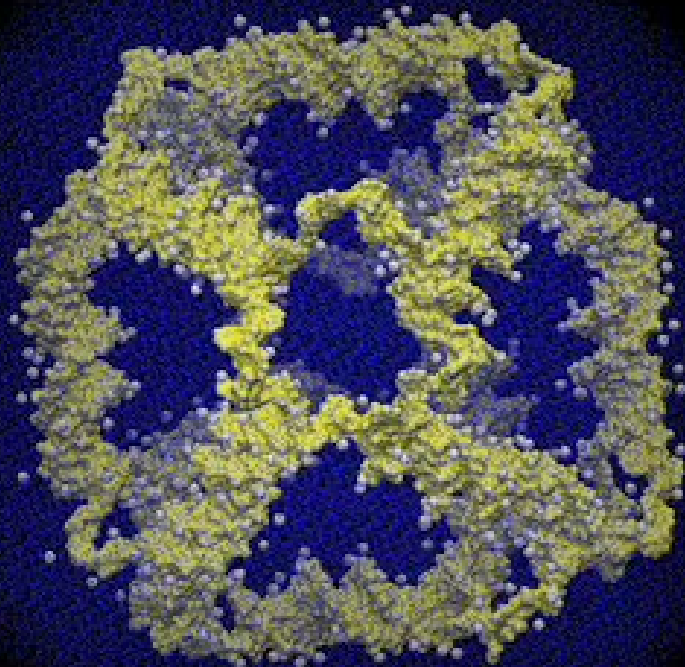
Andersen et. al. 2007

17/04/09

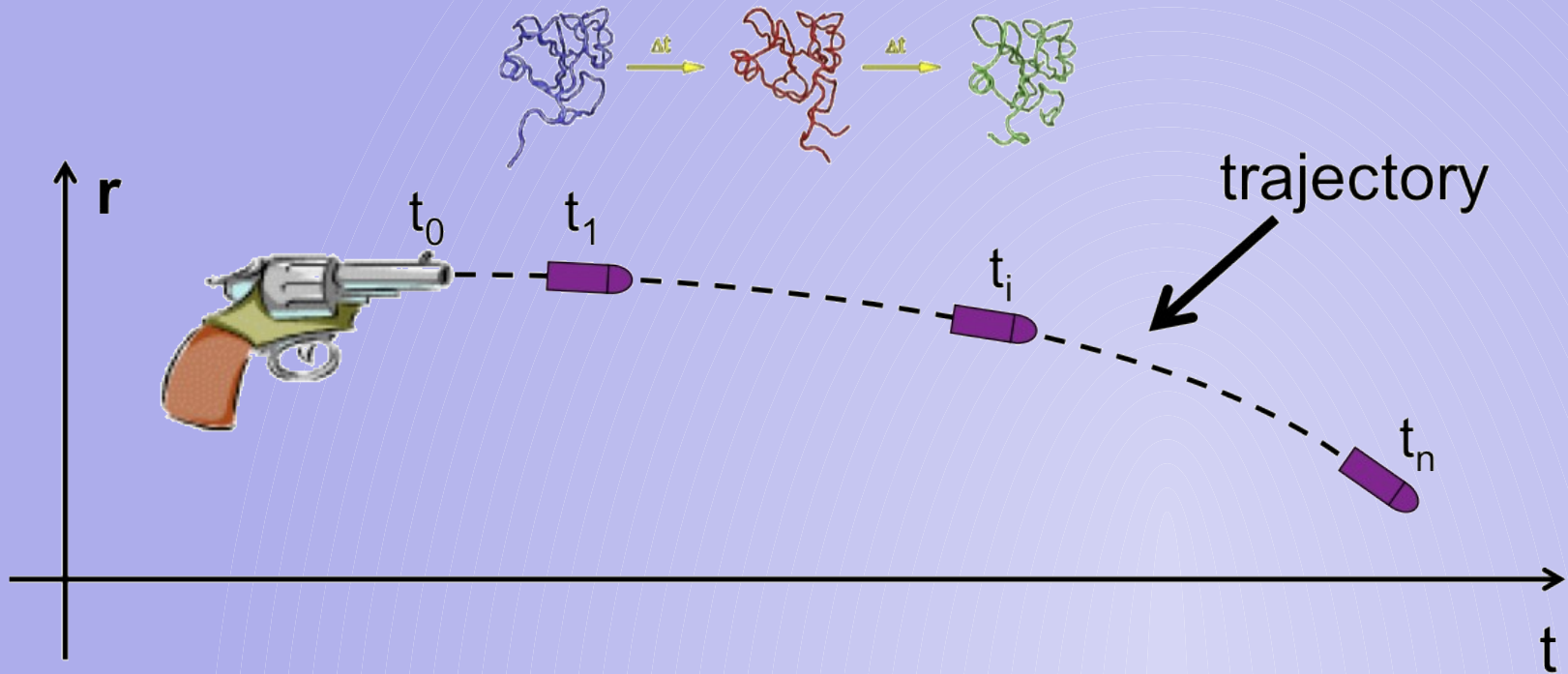
The Nanocage

High Resolution

Total Atoms	3929
DNA atoms	1908
Bases	600
Water molecules	124425
Na ⁺ ions	600
Simulation box side X (Å)	1
Simulation box side Y (Å)	1
Simulation box side Z (Å)	1



Molecular Dynamics Simulation



$$F_i(t) = m_i a_i(t)$$

$$F = -\delta V / \delta r_i$$

$$a_i = -(1/m) \delta V / \delta r_i$$

$$r_i(t + \Delta t) = r_i(t) + v_i(t)\Delta t + 1/2 a_i(t)\Delta t^2$$

$$v_i(t + \Delta t) = v_i(t) + a_i(t)\Delta t$$

Il campo di forze

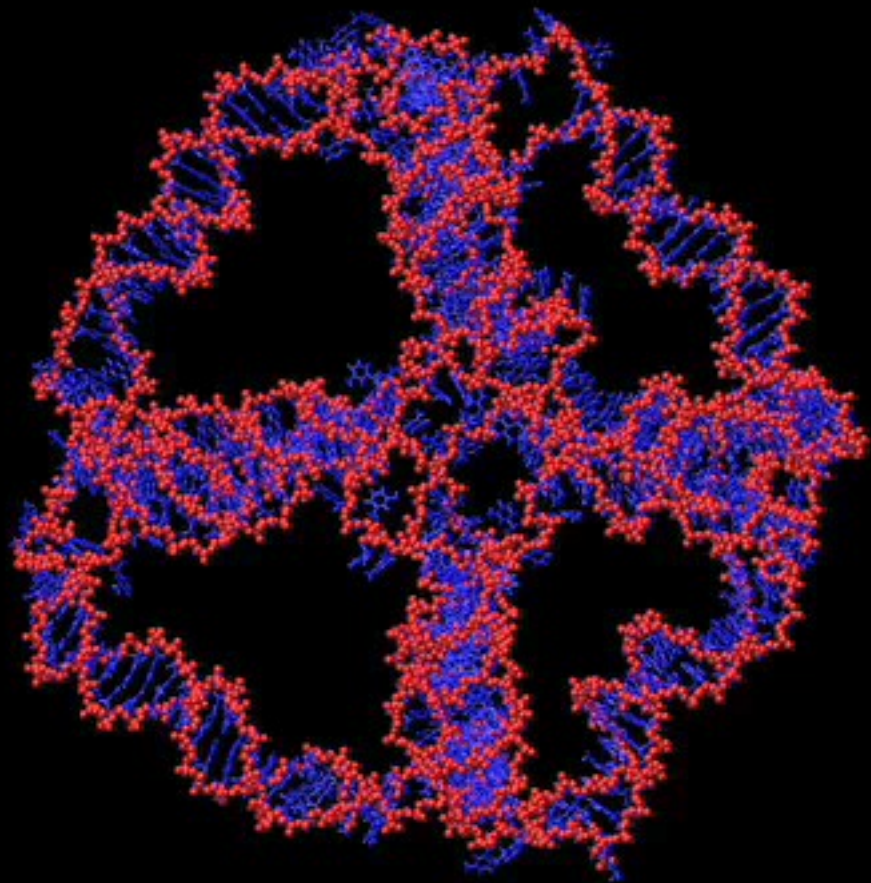
Un potenziale tipico, usato in molti codici di Dinamica Molecolare classica, è la somma di “interazioni di legame” e di “interazioni di non legame”:

Nota che il potenziale è funzione solo delle posizioni delle particelle

$$V(\mathbf{r}_1, \mathbf{r}_2, \dots, \mathbf{r}_n) = \sum_{\text{bond}} \frac{1}{2} k_{b_n} (b_n - b_{0_n})^2 + \sum_{\text{angle}} \frac{1}{2} k_{q_n} (q_n - q_{0_n})^2 +$$
$$+ \sum_{\text{improper dihedral}} \frac{1}{2} k_{x_n} (x_n - x_{0_n})^2 + \sum_{\text{dihedral}} k_{f_n} [1 + \cos(m_n f_n - d_n)] +$$
$$+ \sum_{\text{nonbonded pairs } (ij)} \left(\left(\frac{C_{ij}^{(12)}}{r_{ij}^{12}} - \frac{C_{ij}^{(6)}}{r_{ij}^6} \right) + \frac{1}{4\pi\epsilon_0} \frac{q_i q_j}{e_r r_{ij}} \right)$$

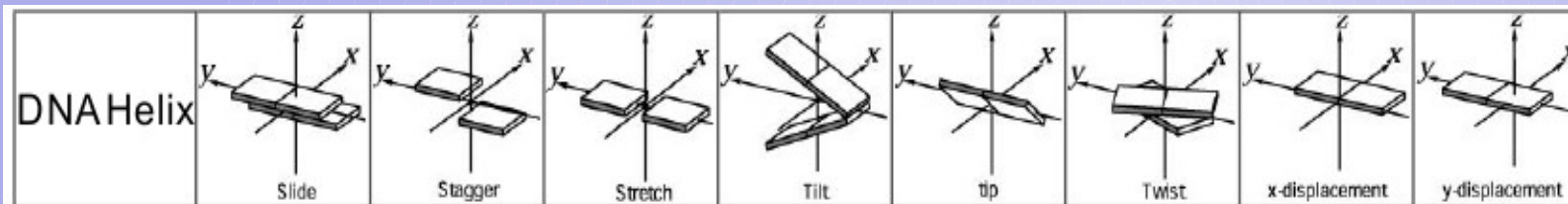
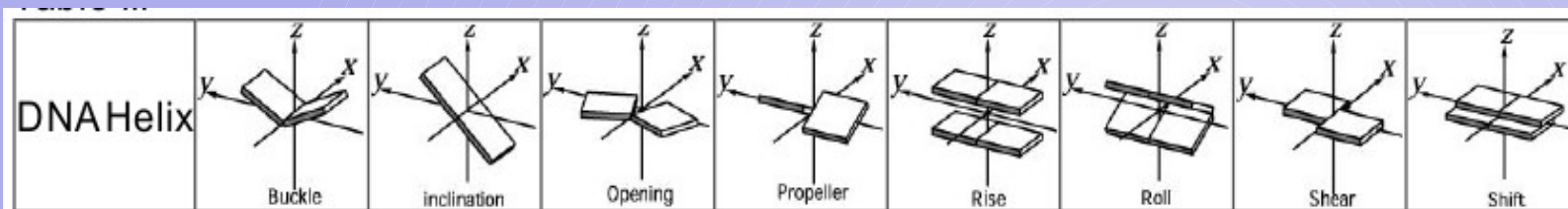
L'ultimo termine comprende le interazioni di non legame

I primi quattro termini rappresentano le interazioni di legame



MD Results

DNA Geometry



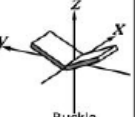
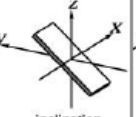
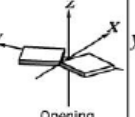
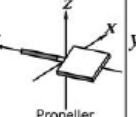
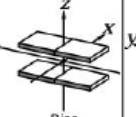
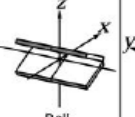
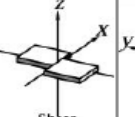
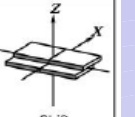
DNA Helix	Sequence	
B-DNA		0.0
DH1	CGATGTCTAAGCTGACCG	17.48 (8.71)
DH2	GGACCGTGATTCCATGAC	33.89 (12.46)
DH3	CTTAGAGTTGCCACCAGG	50.31 (15.57)
DH4	GAATCCTATGCTCGGACG	24.41 (11.43)
DH5	GGCTCACATTGGCTACAG	25.65 (11.05)
DH6	CTATCCGATCGAGGCATG	28.72 (12.16)
DH7	CATACTGAGAGCGTTCCG	19.26 (9.28)
DH8	GTCGCAGTTCAGATACCG	33.21 (13.08)
DH9	CGGTTACGGTACAATGCC	30.87 (14.70)
DH10	CGCAAGACGTTAGTGCC	35.17 (13.74)
DH11	CCACCGAATGGTGATCG	24.34 (11.79)
DH12	GTATGACGCAGCACTTGC	35.41 (13.97)
Average(SD)		12.5(2.16)

17/04/09

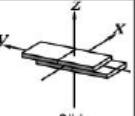
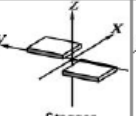
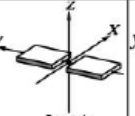
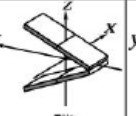
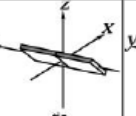
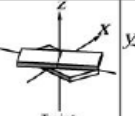
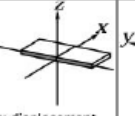
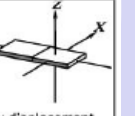
MD Results

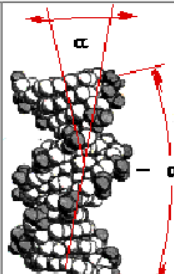
DNA Geometry

Table III

DNA Helix								
	Buckle	Inclination	Opening	Propeller	Rise	Roll	Shear	Shift
B-DNA	0.00	2.74	0.16	-15.07	3.38	0.00	0.00	0.00
DH1	1.52 (13.38)	0.06 (3.43)	3.58 (2.61)	-11.31 (6.27)	3.53 (6.16)	0.45 (3.16)	0.02 (0.27)	-0.01 (0.42)
DH2	-0.83 (4.75)	-1.43 (1.23)	2.70 (1.03)	-8.50 (8.34)	3.73 (6.12)	-0.14 (2.58)	-0.01 (0.14)	0.02 (0.52)
DH3	0.19 (8.11)	-3.43 (2.56)	2.89 (3.16)	-8.82 (5.34)	4.77 (6.98)	-0.00 (2.12)	-0.02 (0.15)	0.00 (0.38)
DH4	-0.89 (6.87)	-2.48 (2.25)	2.72 (1.62)	-10.19 (5.79)	3.90 (6.18)	0.28 (1.96)	-0.01 (0.16)	0.03 (0.25)
DH5	0.52 (8.29)	-2.89 (1.28)	3.19 (1.79)	-9.16 (6.56)	4.00 (5.20)	-0.01 (2.19)	-0.01 (0.15)	-0.03 (0.42)
DH6	0.14 (6.16)	-2.15 (1.44)	2.87 (2.25)	-9.14 (8.25)	4.70 (6.58)	0.08 (2.57)	0.03 (0.15)	-0.02 (0.44)
DH7	-1.38 (7.56)	-0.61 (4.53)	2.80 (1.48)	-9.27 (7.49)	3.74 (6.77)	-0.03 (3.59)	0.03 (0.14)	-0.02 (0.39)
DH8	-0.79 (7.69)	-2.86 (2.26)	2.89 (1.46)	-9.55 (7.39)	3.98 (5.65)	-0.39 (2.46)	-0.00 (0.18)	-0.02 (0.41)
DH9	-1.81 (8.24)	-2.22 (4.51)	3.51 (1.29)	-7.65 (8.54)	3.97 (5.46)	1.03 (2.52)	-0.02 (0.15)	0.04 (0.50)
DH10	0.27 (8.94)	0.70 (4.30)	3.21 (1.91)	-8.76 (8.50)	4.07 (7.14)	0.43 (3.38)	0.00 (0.18)	0.03 (0.38)
DH11	-0.86 (5.67)	-1.66 (2.20)	2.95 (1.56)	-8.79 (6.86)	4.67 (6.25)	0.37 (2.76)	-0.01 (0.14)	0.00 (0.42)
DH12	-0.64 (6.52)	-2.88 (1.54)	3.04 (1.85)	-8.65 (6.55)	4.37 (7.34)	0.11 (2.84)	0.00 (0.14)	0.03 (0.47)

Each double helix, remains in the B-DNA form along the entire trajectory, although small curvature fluctuations are observed

DNA Helix								
	Slide	Stagger	Stretch	Tilt	Tip	Twist	x-displacement	y-displacement
B-DNA	0.00	-0.09	0.01	0.00	0.00	36.00	0.18	0.00
DH1	3.45 (0.33)	-0.16 (0.32)	0.22 (0.11)	-0.16 (0.35)	1.78 (2.81)	33.51 (4.79)	-1.13 (0.19)	-0.01 (0.28)
DH2	3.41 (0.17)	-0.08 (0.11)	0.17 (0.02)	-0.14 (0.24)	-0.92 (3.00)	33.25 (3.27)	-0.74 (0.17)	0.01 (0.29)
DH3	3.42 (0.30)	-0.02 (0.11)	0.16 (0.04)	-0.13 (0.36)	0.07 (2.28)	31.66 (5.94)	-0.64 (0.17)	-0.02 (0.23)
DH4	3.39 (0.22)	-0.02 (0.20)	0.17 (0.03)	-0.10 (0.24)	1.09 (3.48)	33.38 (3.49)	-0.62 (0.15)	-0.04 (0.22)
DH5	3.42 (0.28)	-0.04 (0.12)	0.18 (0.03)	-0.13 (0.28)	0.55 (3.20)	33.58 (3.88)	-0.78 (0.15)	-0.01 (0.25)
DH6	3.40 (0.23)	-0.06 (0.17)	0.17 (0.03)	-0.16 (0.31)	0.05 (3.08)	32.06 (6.69)	-0.59 (0.18)	0.01 (0.31)
DH7	3.38 (0.23)	-0.05 (0.17)	0.18 (0.03)	-0.15 (0.37)	-0.05 (3.48)	33.04 (3.90)	-0.67 (0.17)	-0.06 (0.48)
DH8	3.41 (0.22)	-0.00 (0.13)	0.17 (0.03)	-0.11 (0.22)	-0.74 (2.94)	33.32 (4.23)	-0.54 (0.20)	0.02 (0.22)
DH9	3.46 (0.27)	-0.05 (0.20)	0.17 (0.04)	-0.16 (0.28)	1.90 (2.80)	33.25 (2.15)	-0.73 (0.22)	-0.23 (0.36)
DH10	3.35 (0.26)	-0.05 (0.21)	0.19 (0.03)	-0.16 (0.29)	0.08 (3.99)	32.76 (3.84)	-0.75 (0.17)	-0.06 (0.48)
DH11	3.39 (0.16)	-0.07 (0.11)	0.18 (0.02)	-0.09 (0.26)	0.41 (4.72)	32.86 (3.70)	-0.57 (0.16)	-0.03 (0.22)
DH12	3.40 (0.22)	-0.03 (0.13)	0.17 (0.03)	-0.13 (0.23)	-0.30 (3.24)	32.96 (3.32)	-0.69 (0.19)	-0.02 (0.26)
Average(SD)	-0.38	-1.82	3.03	-9.15	4.12	0.18	0.00	0.01

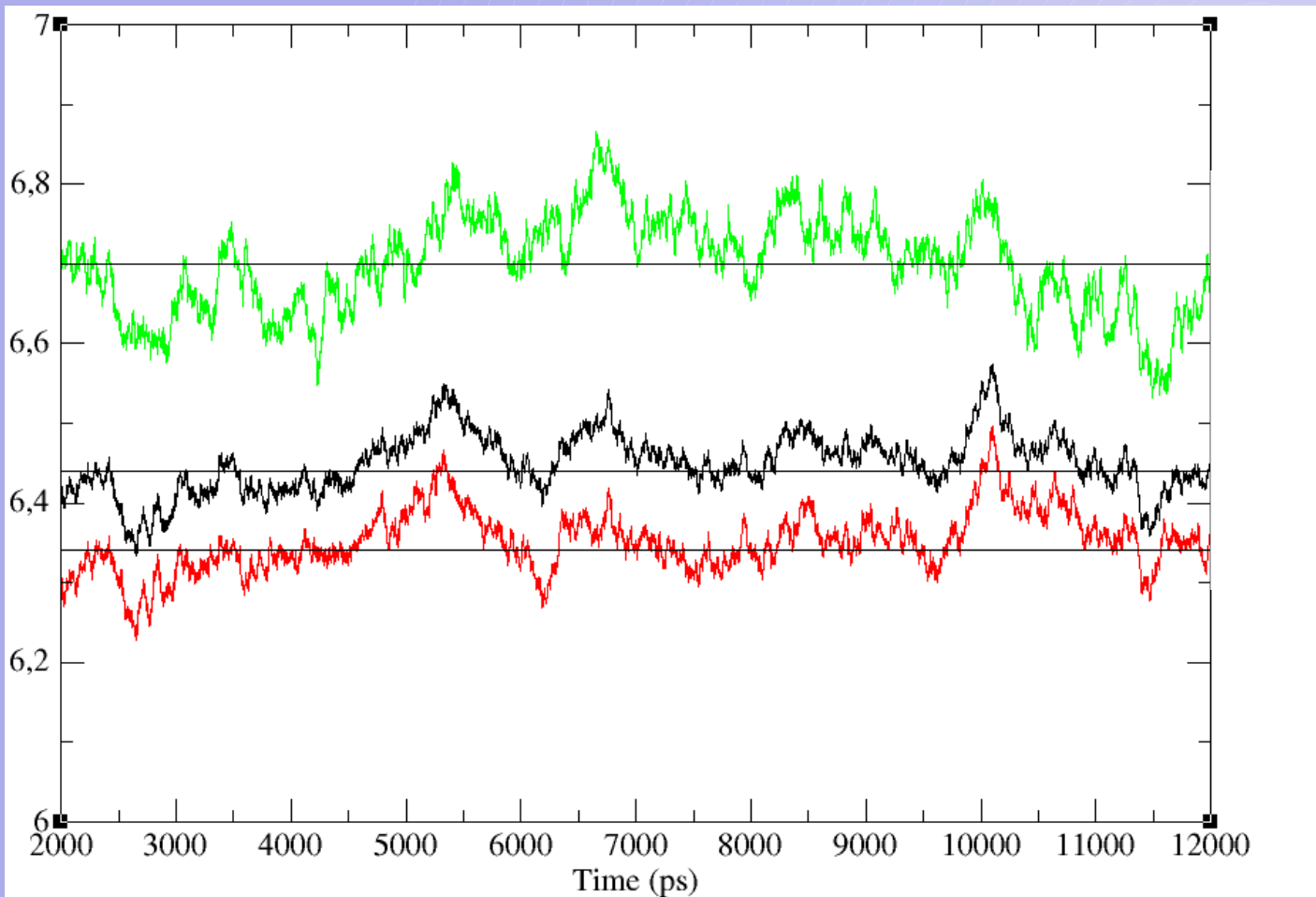
DNA Helix	Sequence	
B-DNA		0.0
DH1	CGATGTCTAAGCTGACCG	17.48 (8.71)
DH2	GGACCGTGATTCCATGAC	33.89 (12.46)
DH3	CTTAGAGTTGCCACCAGG	50.31 (15.57)
DH4	GAATCCTATGCTCGGACG	24.41 (11.43)
DH5	GGCTCACATTGGCTACAG	25.65 (11.05)
DH6	CTATCCGATCGAGGCATG	28.72 (12.16)
DH7	CATACTGAGAGCGTTCCG	19.26 (9.28)
DH8	GTCGAGTTCAGATACCG	33.21 (13.08)
DH9	CGGTACGGTACAATGCC	30.87 (14.70)
DH10	CGAAGACGTTAGTGTCC	35.17 (13.74)
DH11	CCACCGAATGGTGTATCG	24.34 (11.79)
DH12	GTATGACGCAGCACTGC	35.41 (13.97)
Average(SD)		12.5 (2.16)

MD Results

Gyration Radius

$$R_g = \sqrt{\frac{N}{\sum_{i=0}^N m_i / M}}$$

	Diameter (nm) Dens.map	Diameter (nm) model
Outer	20	19
Inner	15	13



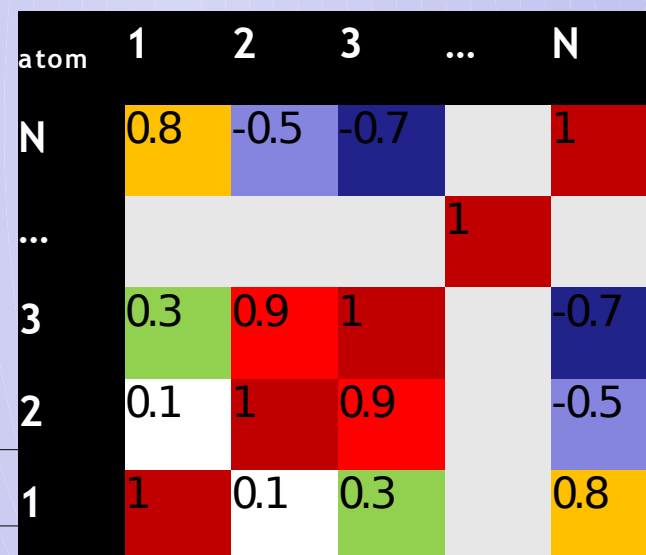
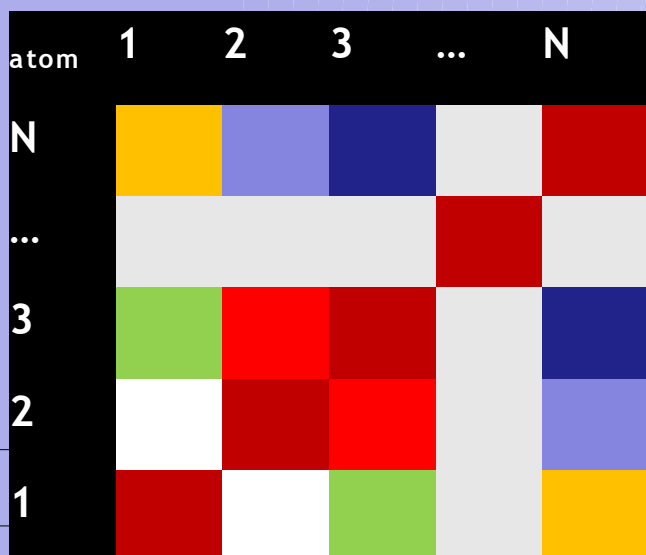
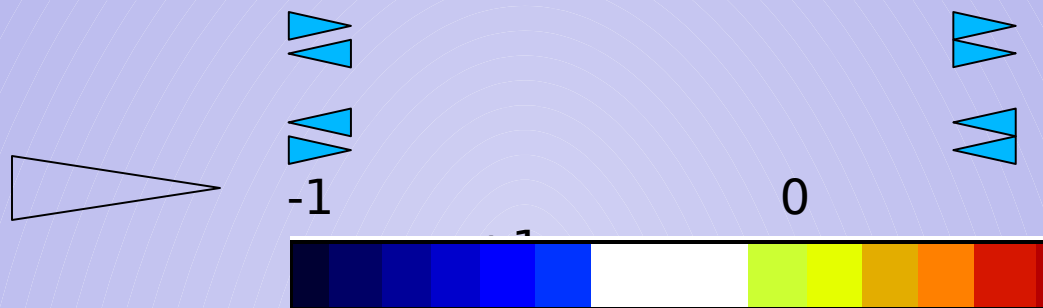
= 13,4
nm

= 12,88
nm
= 12,68
nm

MD Results

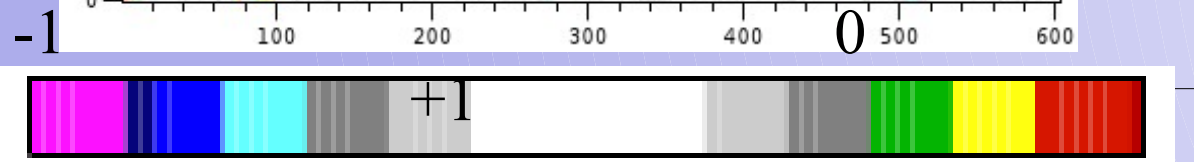
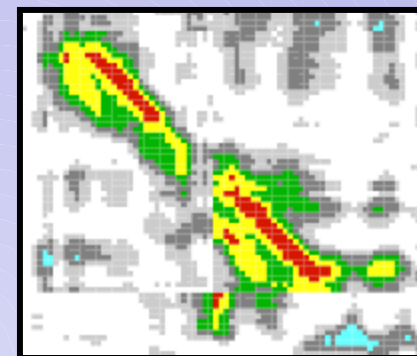
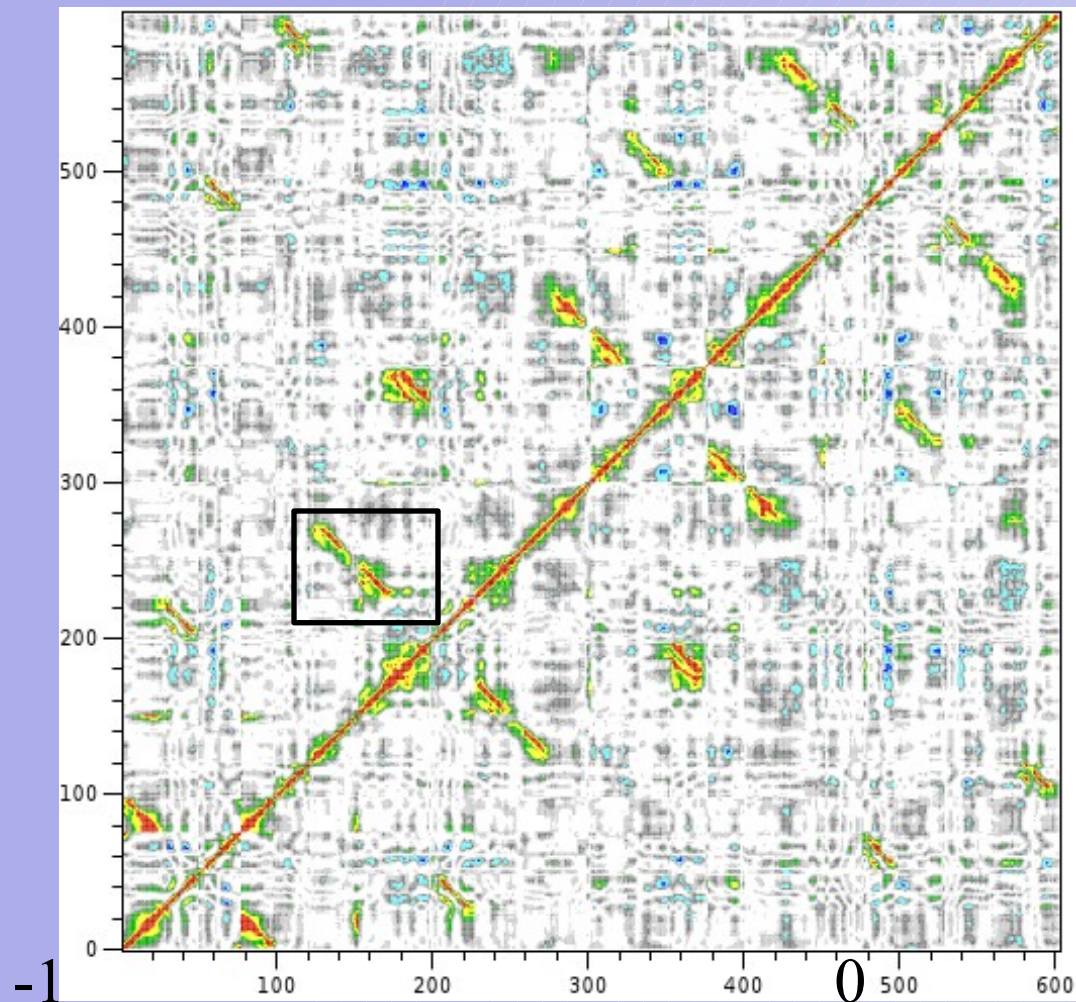
Correlation Map

atom	1	2	3	...	N
N	0.8	-0.5	-0.6		1
...				1	
3	0.3	0.9	1		-0.6
2	0.1	1	0.9		-0.5
1	1	0.1	0.3		0.8



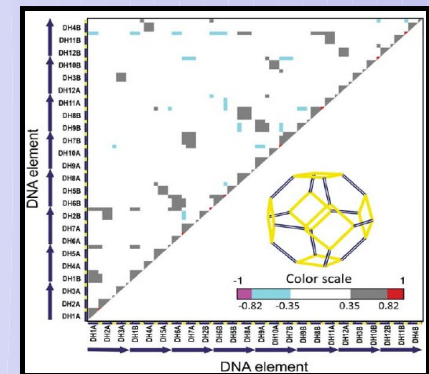
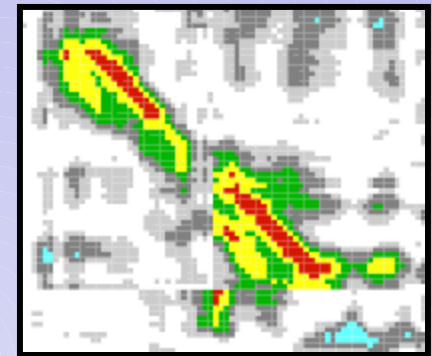
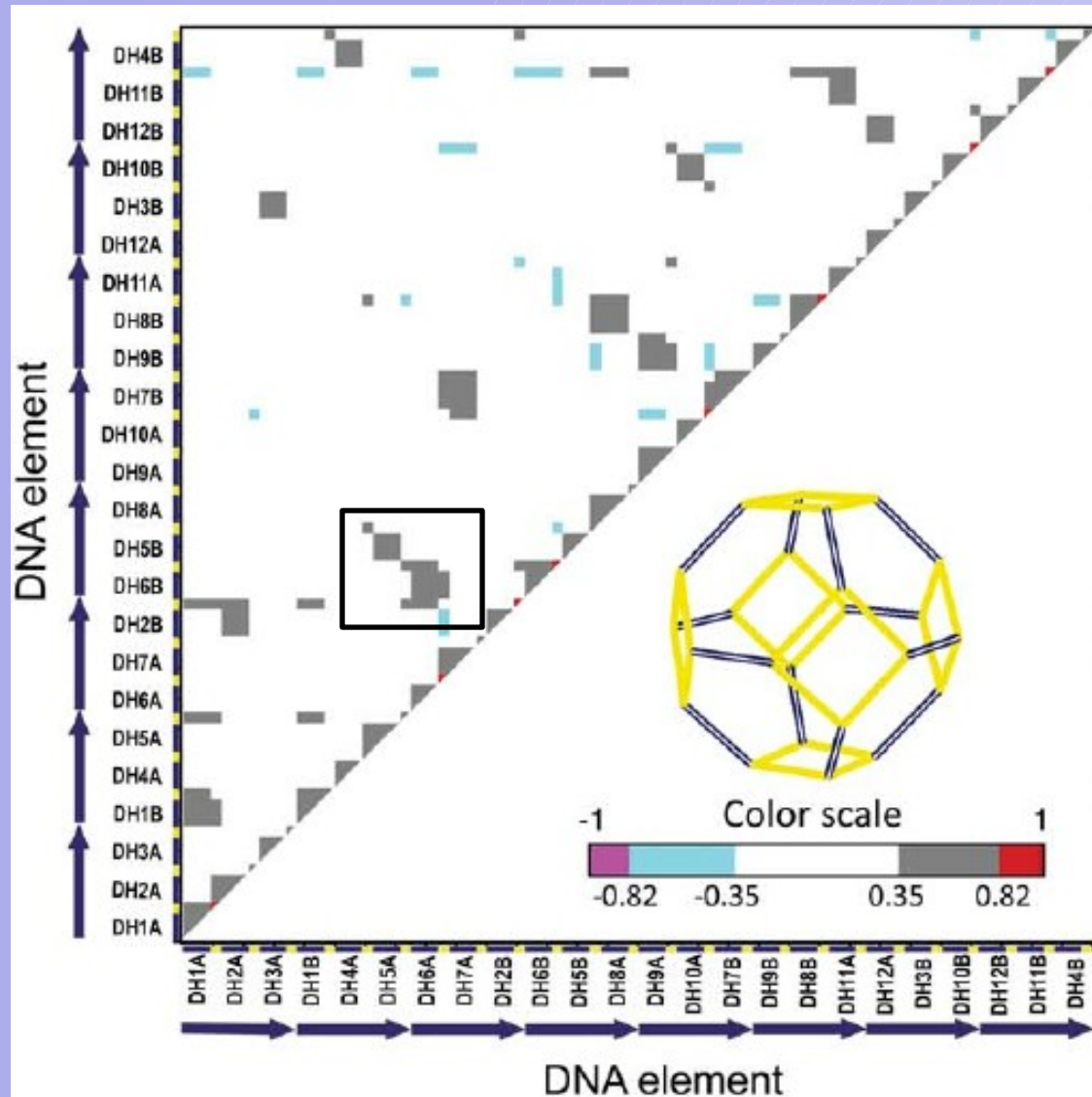
MD Results

Correlation Map



MD Results

Correlation Map



MD Results

Correlation Map

2 type of segment:

Double Helix single strand (DHss)

Thymidine Bridge single strand (TBss)

3 couple type Double helix single strand

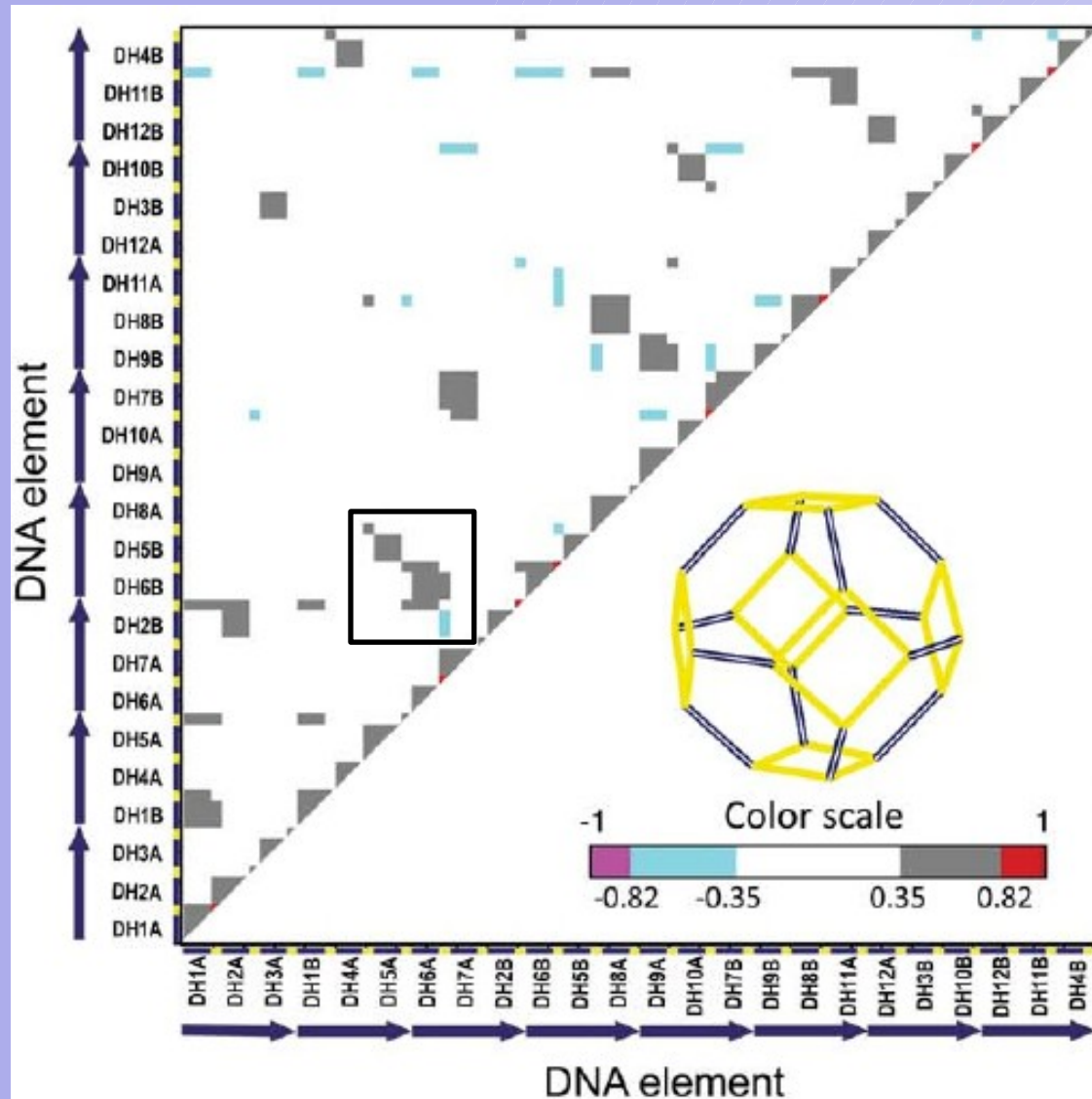
a) DHss vs DHss

b) DHss vs TBss

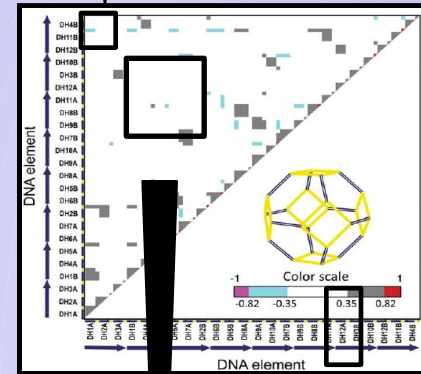
c) TBss vs TBss

MD Results

Correlation Map



Thymidine Single strand
VS
Thymidine Single strand

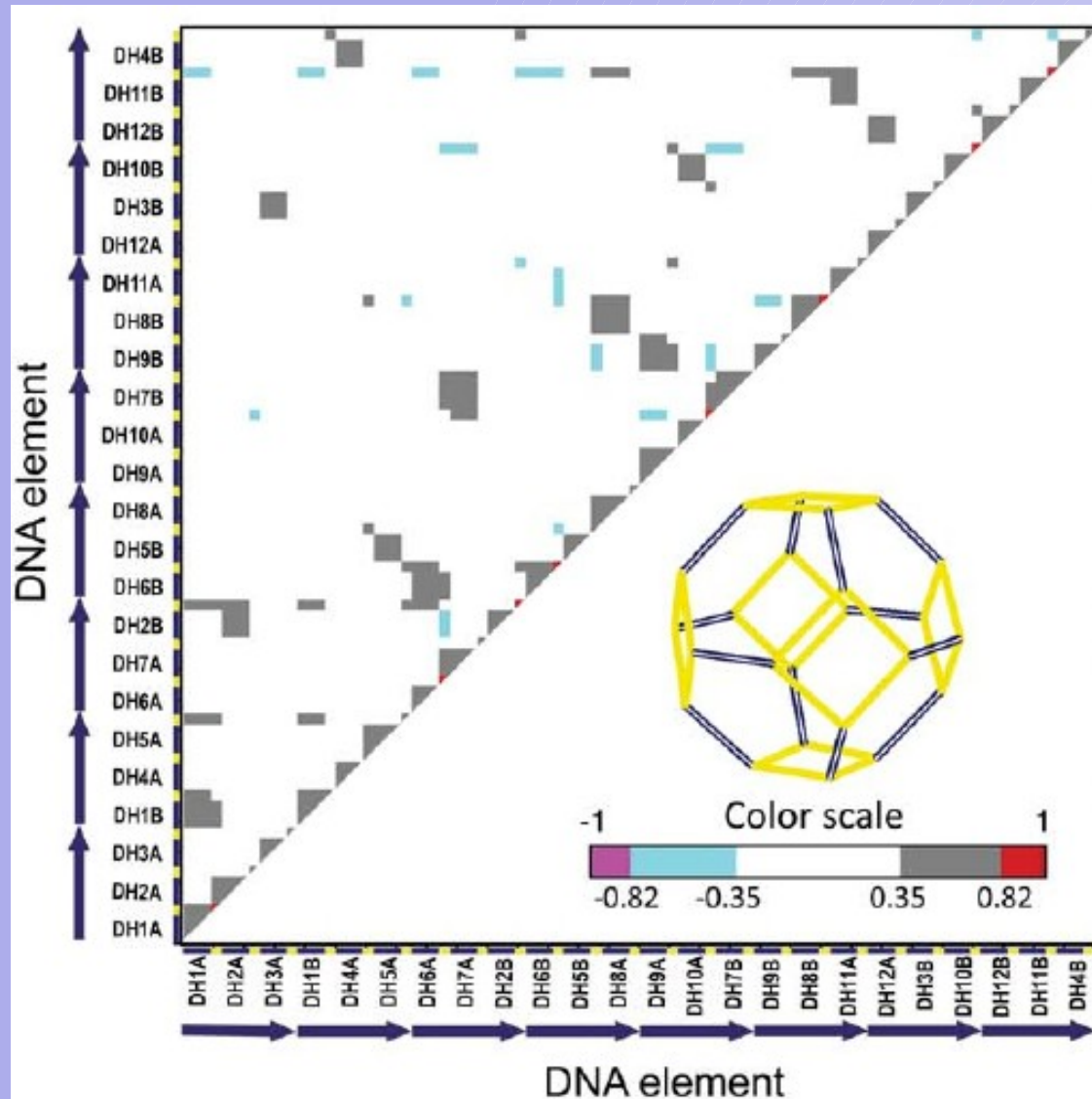


DH Single strand
VS
Thymidine Single strand

DH Single strand
VS
DH Single strand

MD Results

Correlation Map



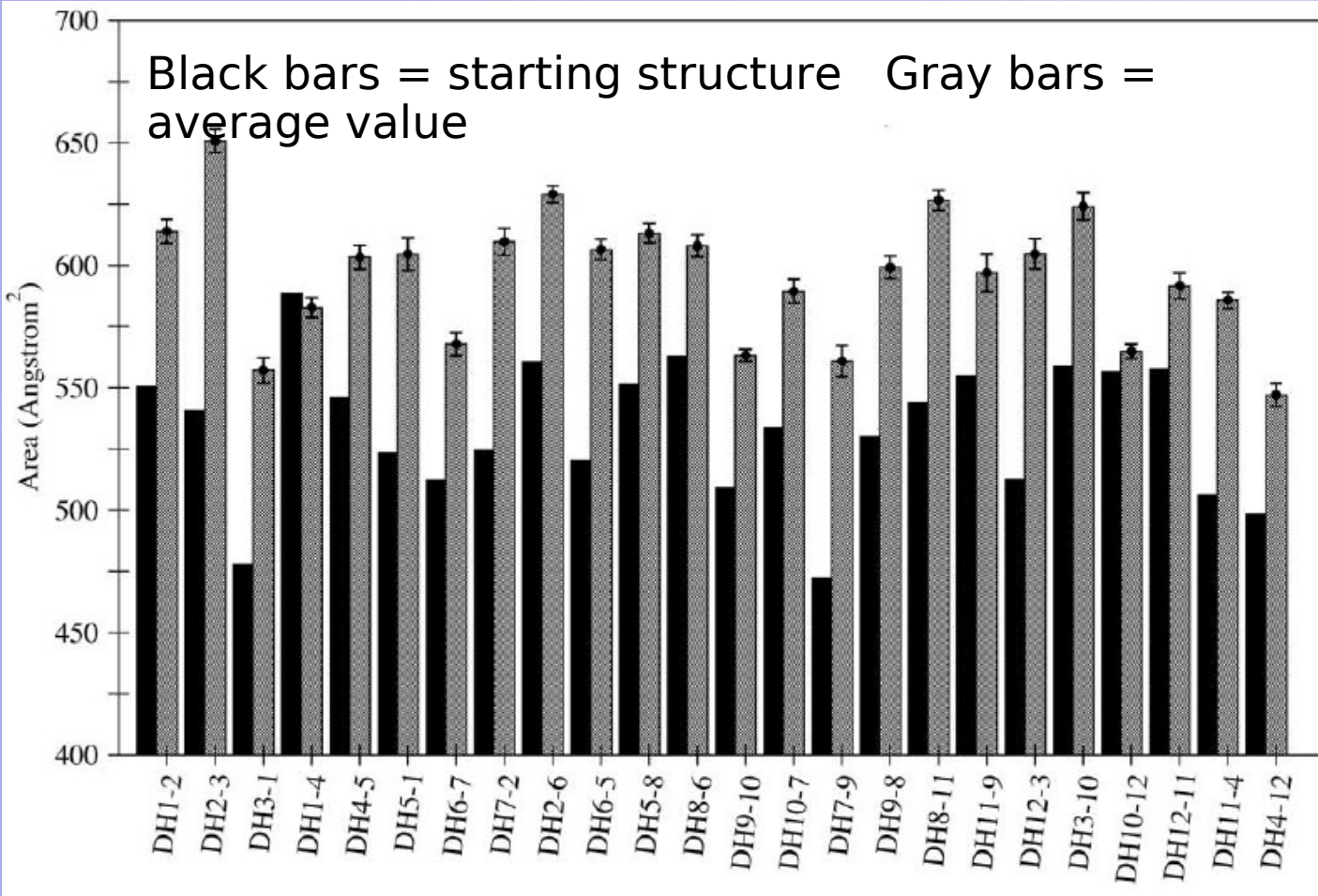
The positive correlated elements (gray spots) are directly connected

The negative correlated elements (cyan spots) are not directly connected, indicating that

THE STRUCTURE IS CONTRACTING

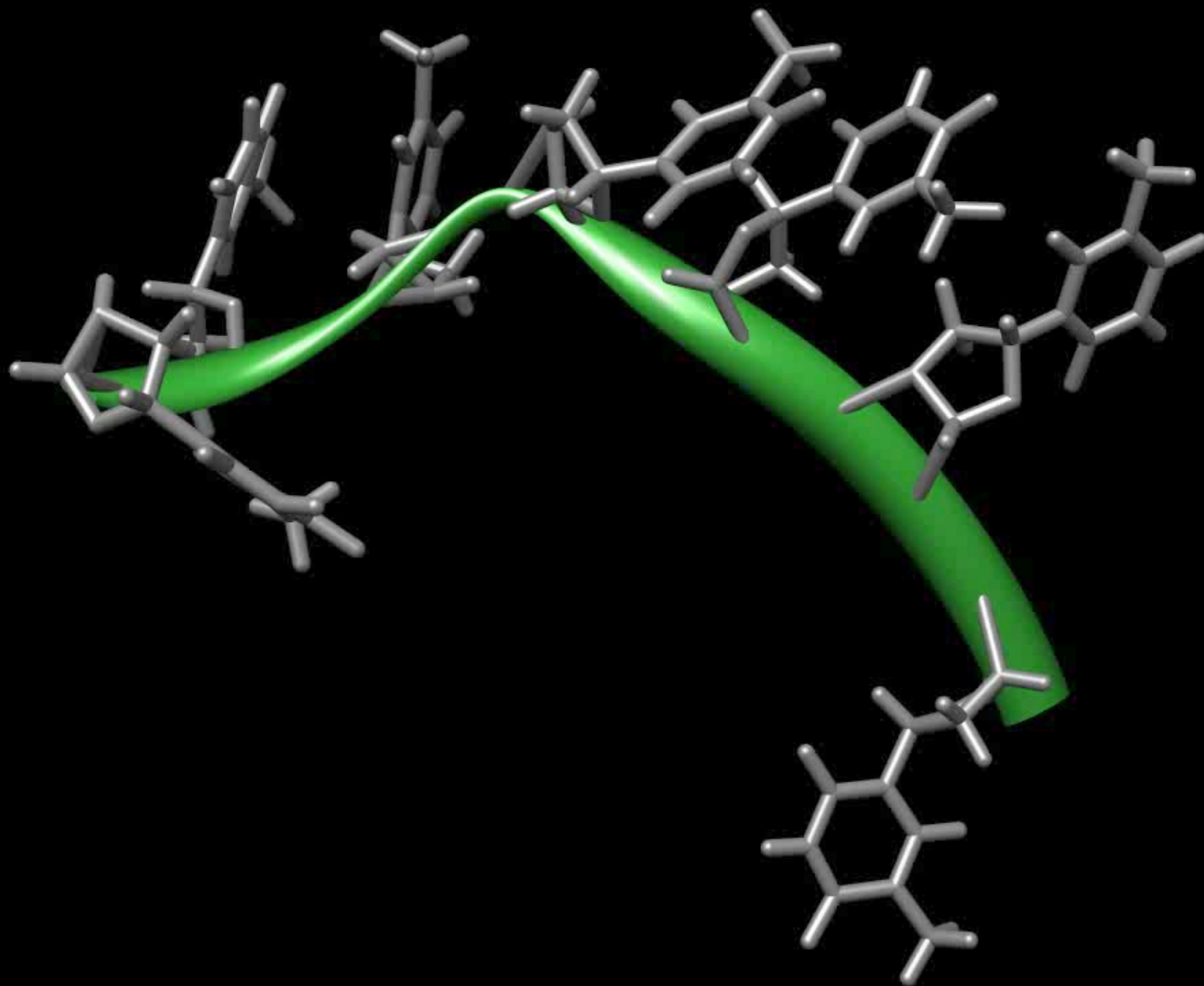
MD Results

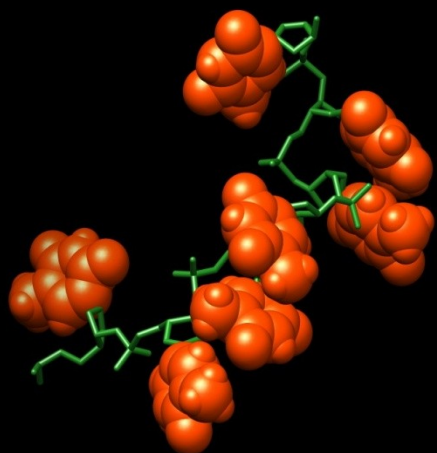
thymidine Strands Contact Surface Evolution



The buried area of the thymidine strands increase along the trajectory minimizing the exposed hydrophobic surface

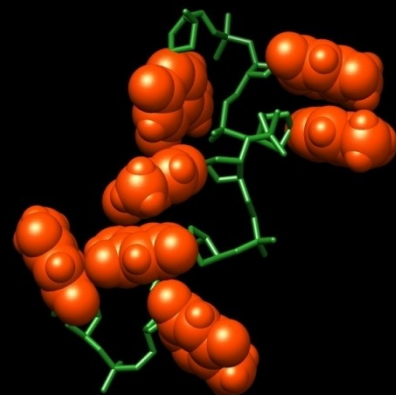
575.62





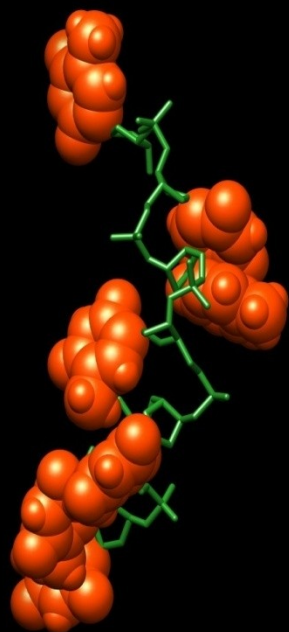
BS(0 ns) = 575

A2



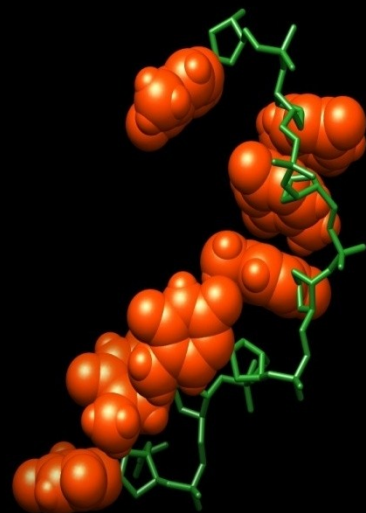
BS(2.2 ns) = 605

A2



17/04/09 BS(5.4 ns) = 617

A2

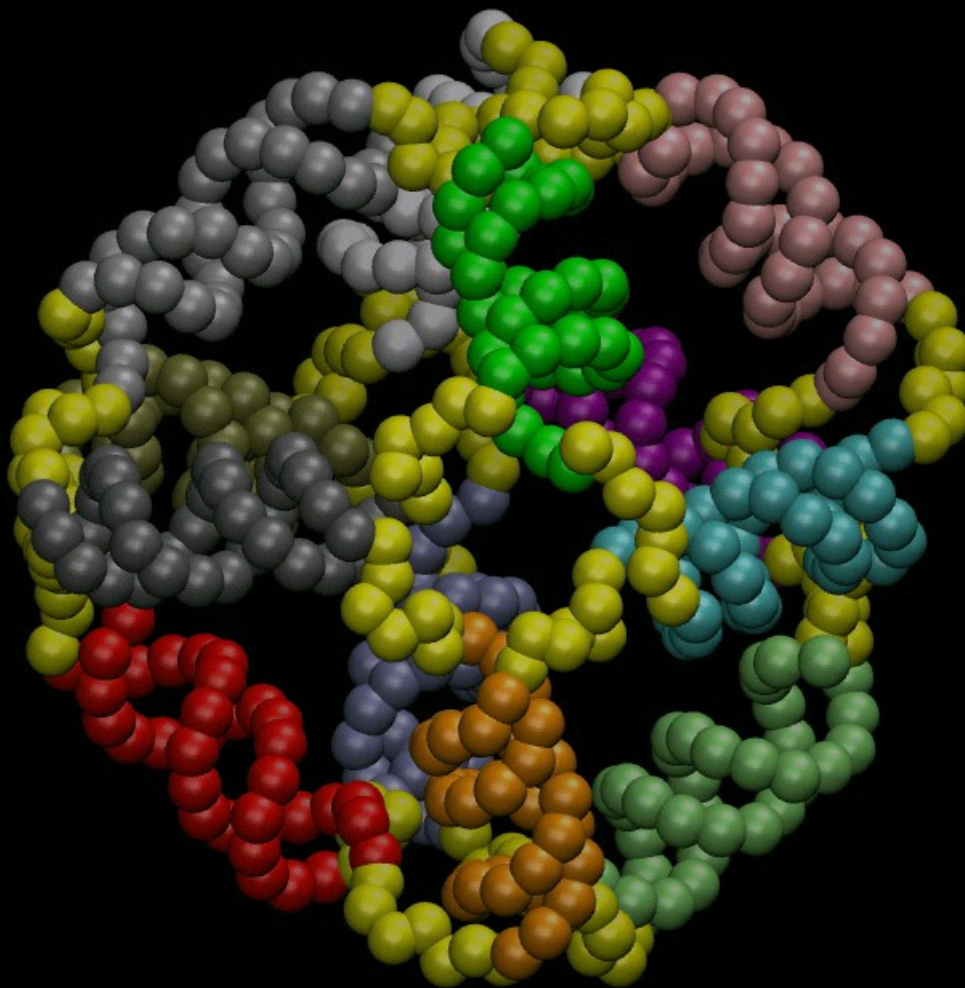


BS(10 ns) = 650

A2

MD Results

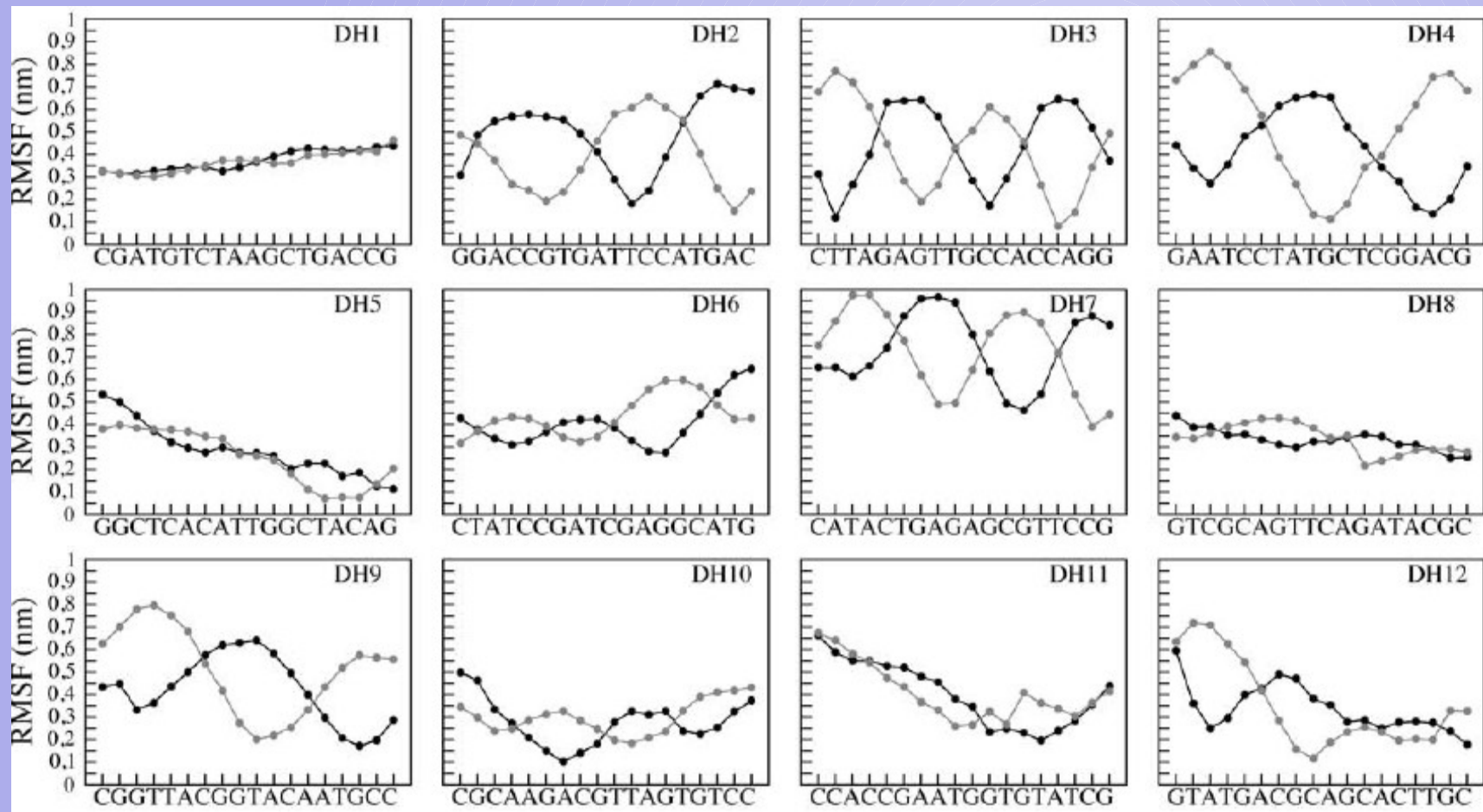
Principal Component Analysis (PCA)



17/04/09

MD Results

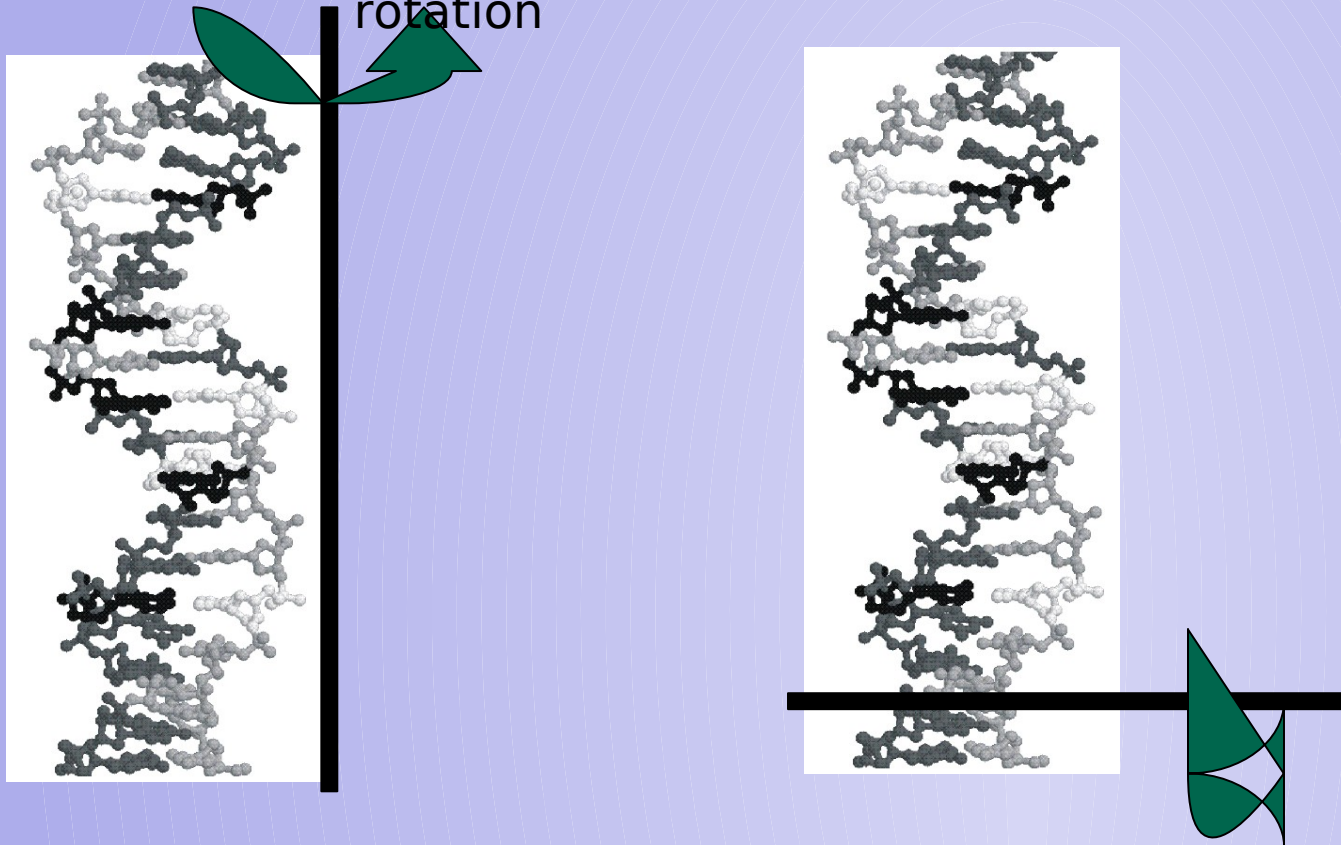
RMSF on the first eigenvector



MD Results

Principal Component Analysis (PCA)

Two different kind of rotation



Axis of rotation flanking

Axis of rotation parallel to one extreme base pair of the double helix

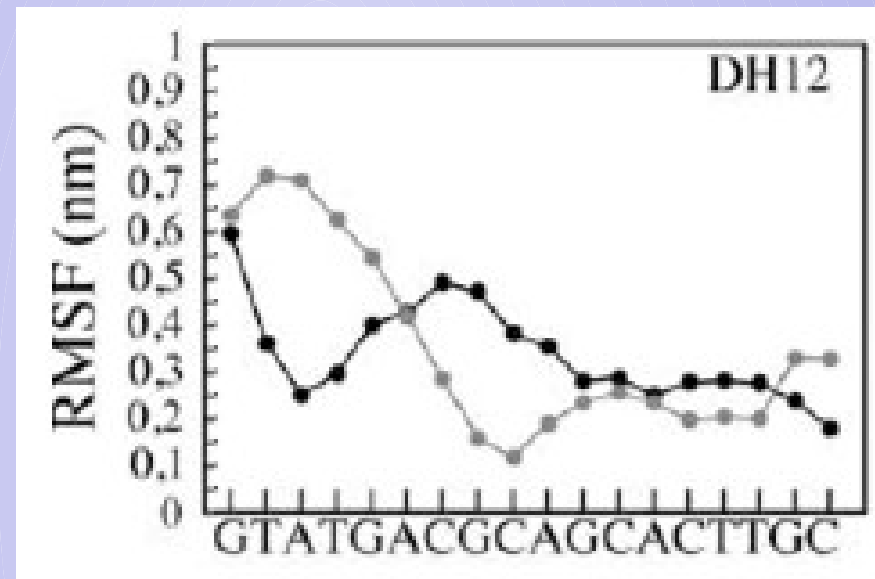
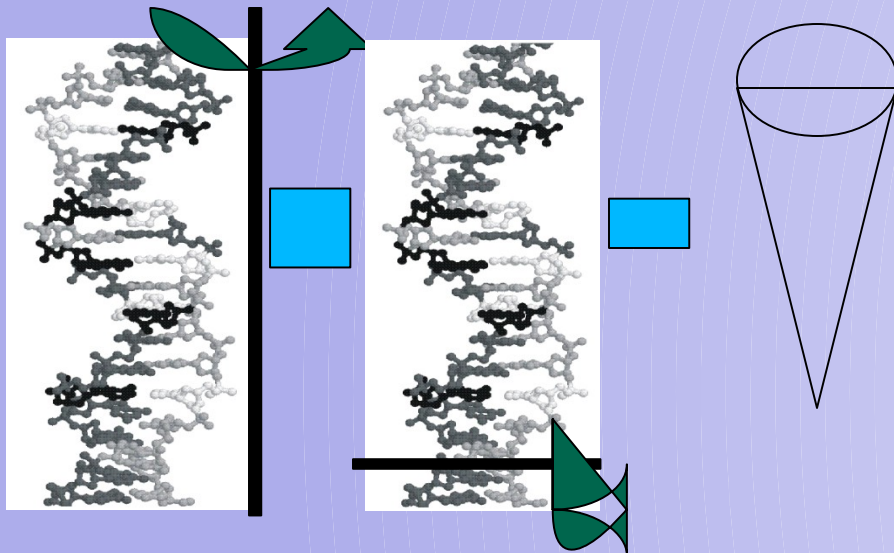
17/04/09

one side of the double helix

MD Results

Principal Component Analysis (PCA)

$$= \sqrt{\frac{1}{n} \sum_{i=1}^n \|v_i - w_i\|^2}$$

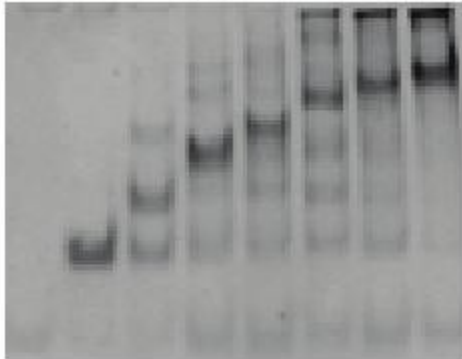


Self-assembling specificity

different thymidine strand length influence

A

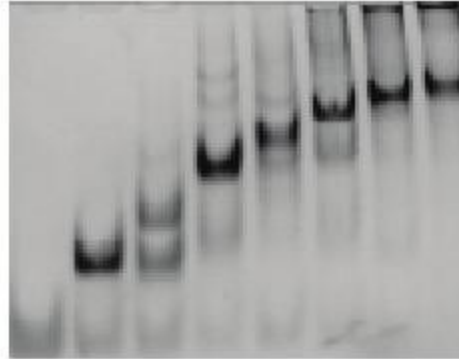
Cage(7T)



1 2 3 4 5 6 7 8

B

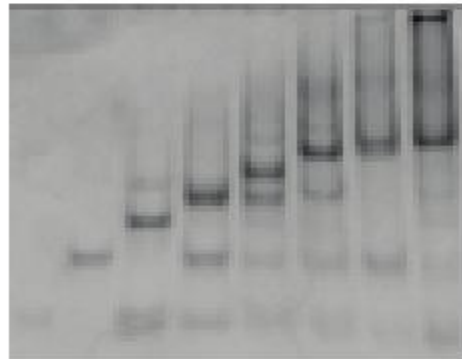
Cage(5T)



1 2 3 4 5 6 7 8

C

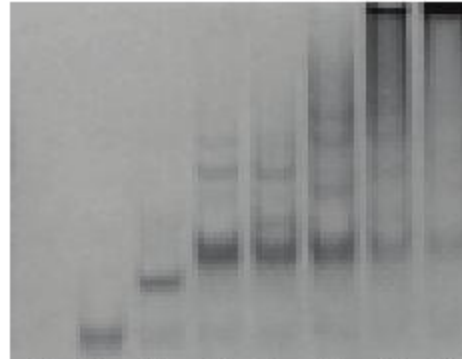
Cage(3T)



1 2 3 4 5 6 7 8

D

Cage(2T)



1 2 3 4 5 6 7 8

The longest are the thymidine strands,



The easiest is the self-assembling

Conclusions

The stability of the global structural parameters as such as DNA geometry, show that the nano-cage structure is maintained in solution.

The global stability is influenced by the thymidine strands behavior

The cage can be used as an holder to protect protein from proteases and simultaneously permits their interaction with molecules small enough to pass through the apertures of the lattice



DECIPHERING THE STRUCTURAL PROPERTIES THAT CONFER STABILITY TO A DNA NANO-CAGE

- M. Falconi F. Oteri
- G. Ghillemi
- B. Knudsen F Andersen
D Tordrup
- JS Pedersen CLP Oliveira
iNANO

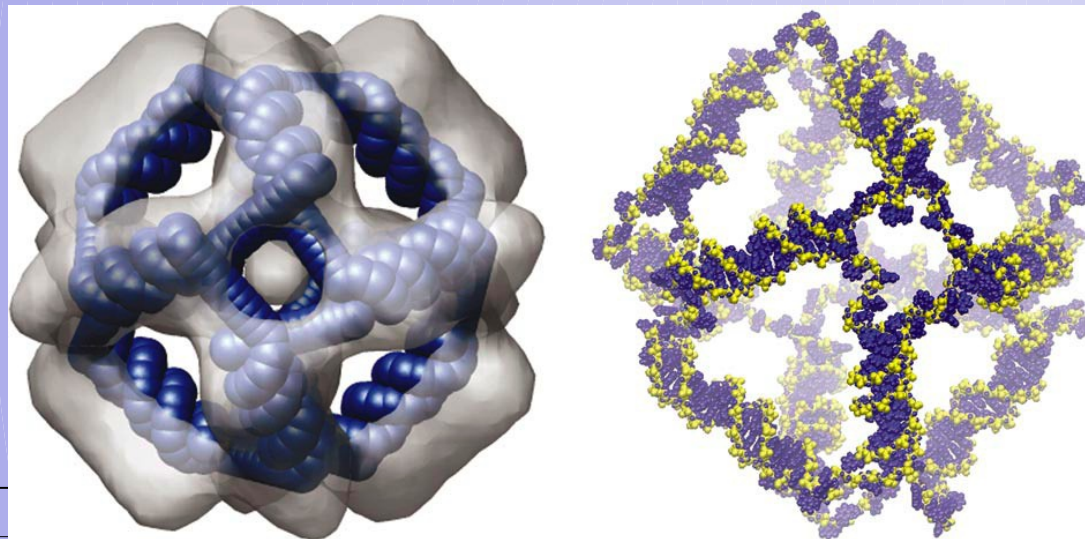
Dip. Biol Tor Vergata NAST

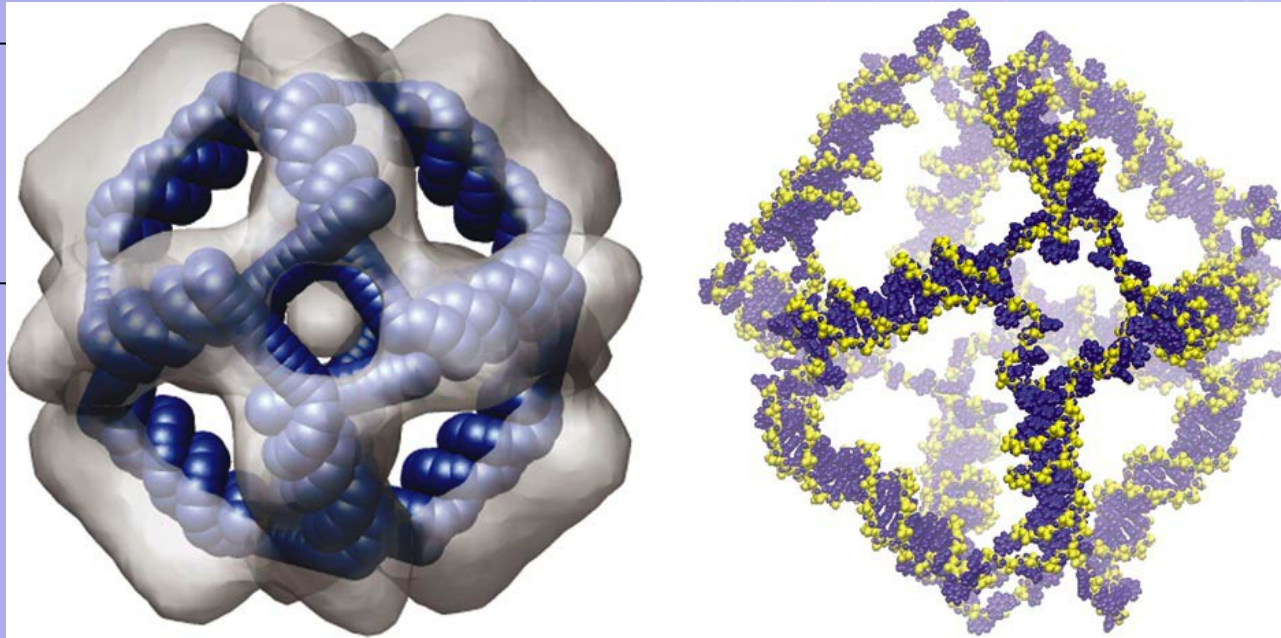
Caspur

Dept Mol Biol. Aarhus Univ.

iNANO

Dept. Chem. Aarhus Univ.





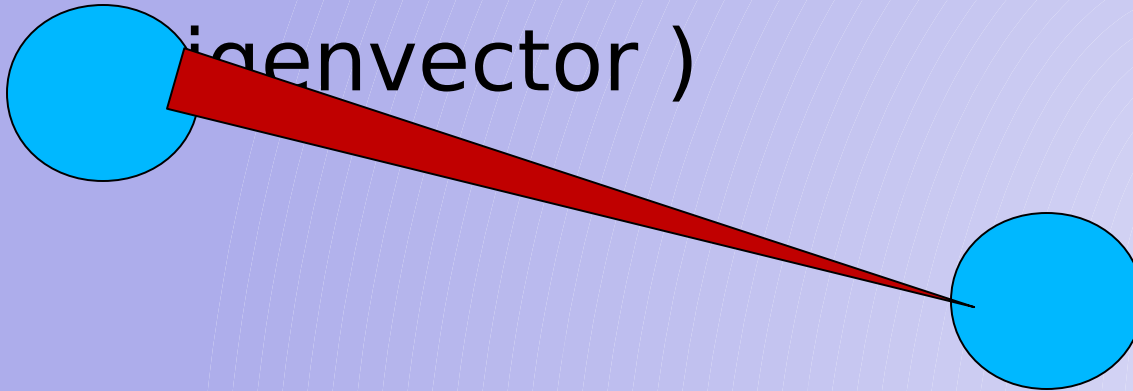
- **Mattia Falconi,†,‡ Francesco Oteri,† Giovanni Chillemi,§ Felicie F. Andersen, David Tordrup,**
- **Cristiano L. P. Oliveira,¶ Jan S. Pedersen,¶ Birgitta R. Knudsen, and Alessandro Desideri,‡,***
- †Department of Biology and Center of Biostatistics and Bioinformatics, University of Rome “Tor Vergata”, Via della Ricerca Scientifica 1, 00133 Rome, Italy, ‡NAST
- Nanoscience & Nanotechnology & Innovative Instrumentation, University of Rome “Tor Vergata”, Via della Ricerca Scientifica 1, 00133 Rome, Italy, §CASPUR Inter-
- University Consortium for the Application of Super-Computing for Universities and Research, Via dei Tizii 6, Rome 00185, Italy, Department of Molecular Biology and
- Interdisciplinary Nanoscience Center (iNANO), Aarhus University, C.F. Møllers Alle´, Bldg. 130, 8000 Aarhus C, Denmark, and ¶Department of Chemistry and

• **17/04/09** Interdisciplinary Nanoscience Center (iNANO), Aarhus University, Langelandsgade 140, 8000 Aarhus C, Denmark

MD Results

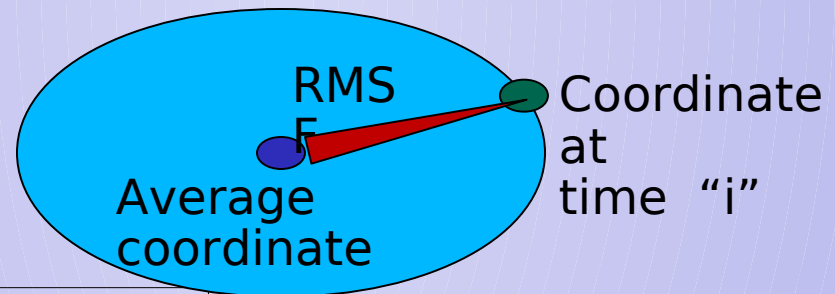
Principal Component Analysis (PCA)

1. Essential motion extraction (eigenvector)



1. Position Standard Deviation

$$\text{RMSF} = \sqrt{\frac{1}{n} \sum_{i=1}^n \|u_i - w_i\|^2}$$



MD Results

Correlation Map

$$\text{Corr}(x, y) = \frac{n \sum x_i y_i - \sum x_i \sum y_i}{\sqrt{n \sum x_i^2 - (\sum x_i)^2} \sqrt{n \sum y_i^2 - (\sum y_i)^2}}$$

$$-1 \leq \text{Corr}(x, y) \leq +1$$

x, y considered atoms

x_i = atoms x position at time i
 y_i = atoms y position at time i

$\text{Corr}(x, y) > 0 \rightarrow$ the atoms moves in the same direction

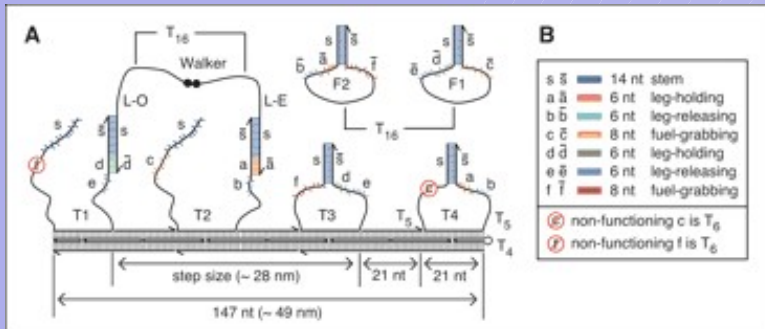


$\text{Corr}(x, y) < 0 \rightarrow$ the atoms moves in the opposite direction

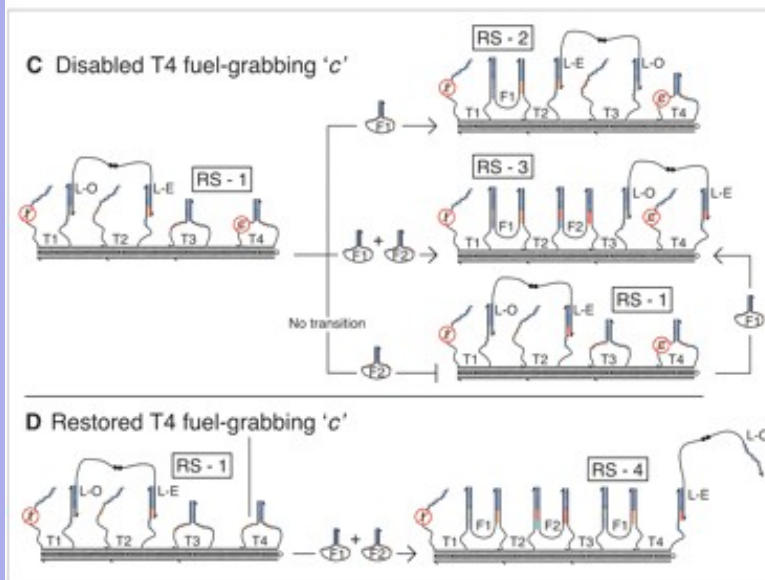


$\text{Corr}(x, y) = 0 \rightarrow$ the atoms moves in uncorrelated direction

A Bipedal DNA Brownian Motor with Coordinated Legs



The walker is a single strand of DNA containing a 5',5' linkage in the middle; one leg is called Leg-Even (L-E), and the other is called Leg-Odd (L-O). The walker walks upon a linear double-crossover (DX) (14) track, which is designed to be approximately 49 nm long and has a persistence length of 100 nm (15). The track is assembled from 18 strands, four of which are metastable stem-loop structures (T1, T2, T3, and T4) that function both in the operation of the device and as structural elements in the track [supporting online material (SOM) text and fig. S1]. Two metastable hairpin fuel strands, F1 and F2, float freely in solution



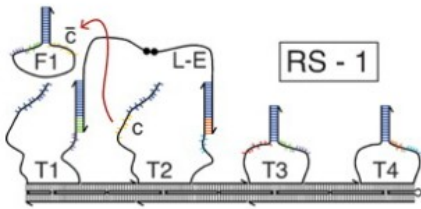
(A) Illustration of the DX track structure with the walker on it. The walker is shown on stem loops T1 and T2. The walker's 5',5' linkage is denoted by two black dots and its 3' ends by half arrows. T16 denotes flexible polythymidine linkers on the walker and two fuel hairpins, F1 and F2. Two T5 regions provide flexibility at the base of the track stem loops. All the binding sites are labeled with lowercase letters, and complementary sequences are capped with a bar. The two fuel-grabbing sequences f and c on T1 and T4, respectively, are not functional.

(B) Color-coding and the names of the binding sites.

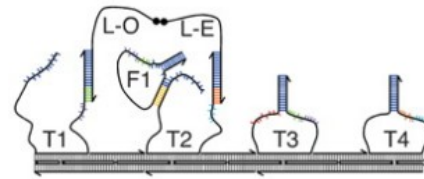
(C) Transitions made with a nonfunctional T4 fuel-grabbing sequence c. The walker is programmed to take two steps from RS-1 to RS-3 with the addition of F1 and F2 simultaneously (middle). A single step is made from RS-1 to RS-2 with the addition of F1 alone (top). With the addition of F2 alone, the walker does not move, and only with the further addition of F1 does the walker make the transition from RS-1 to RS-3 (bottom).

(D) With the T4 fuel-grabbing sequence c restored, the walker transitions to RS-4, incorporating another F1 into the track, thereby kicking L-O off of T3

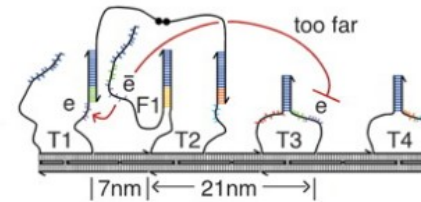
1. L-E leads. T2 is activated and ready for F1.



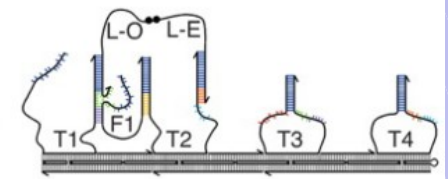
2. T2 invades F1.



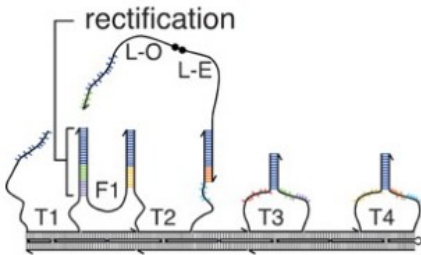
3. F1 is activated by T2.



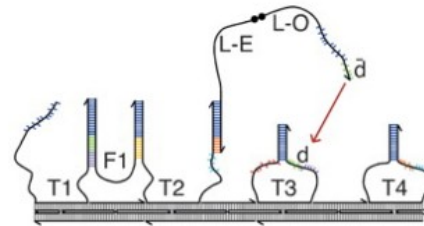
4. F1 invades T1.



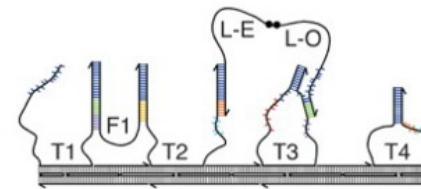
5. L-O is freed by F1.



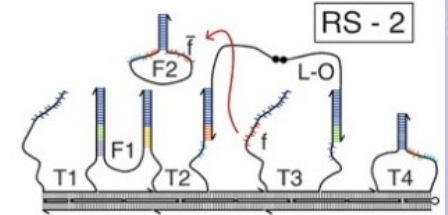
6. L-O diffuses to T3.



7. L-O invades T3.

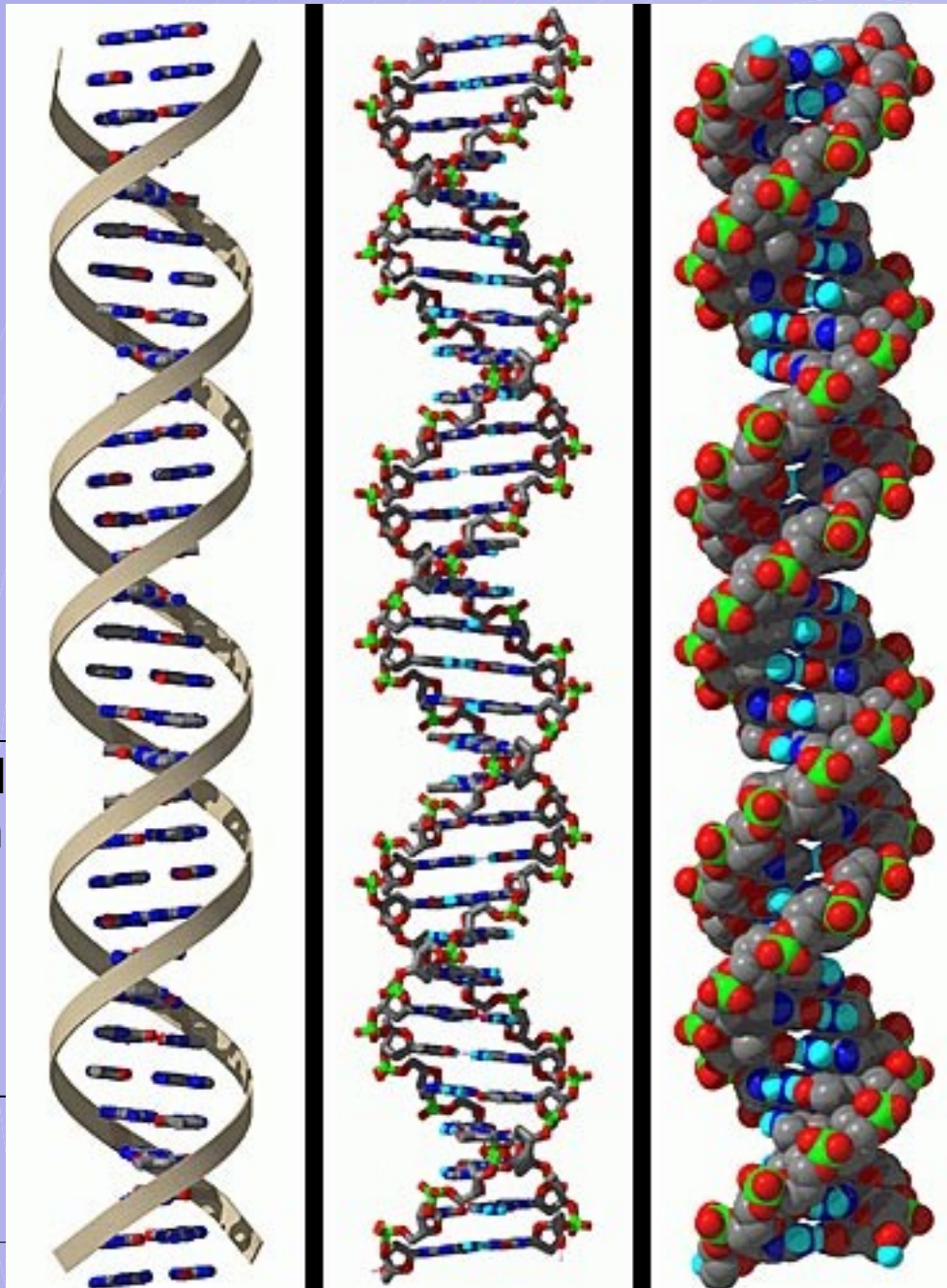


8. L-O leads. T3 is activated and ready for F2.



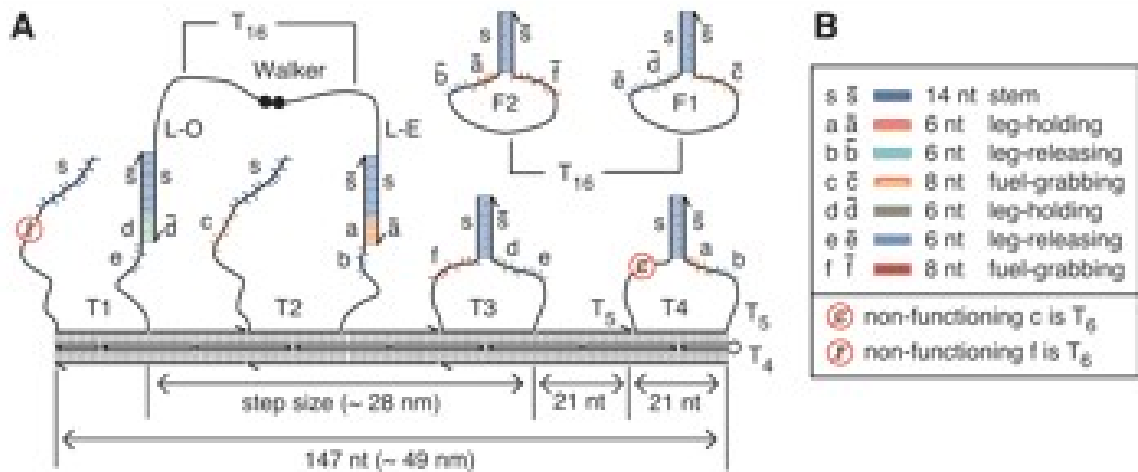
17/04/09

Fare cl
schem

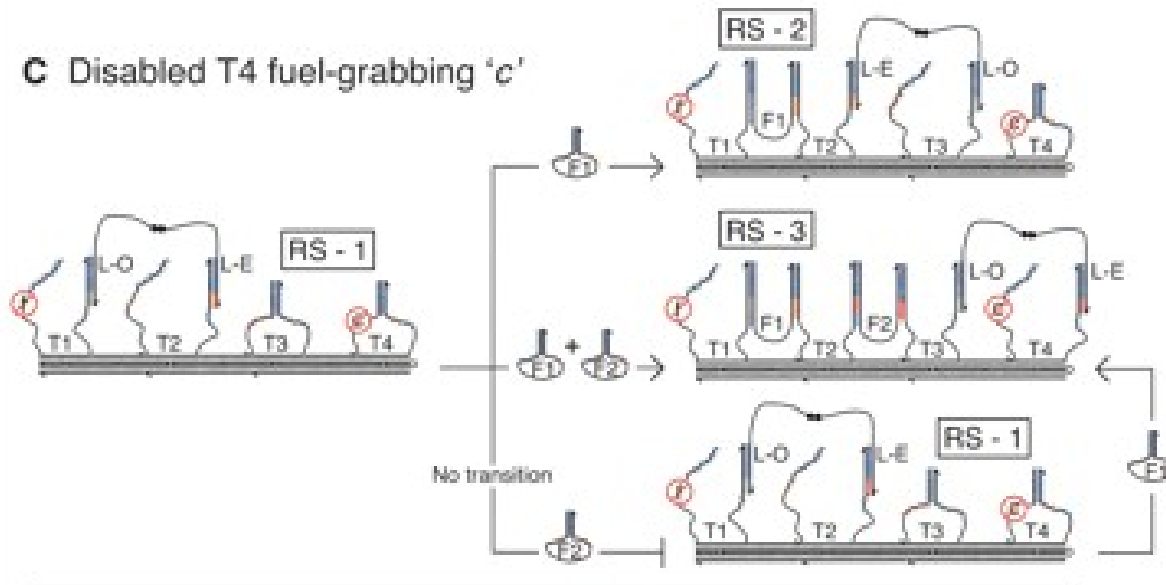


ello

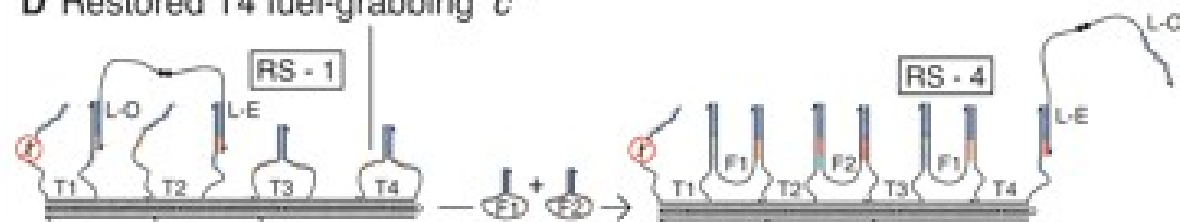
17/04/09



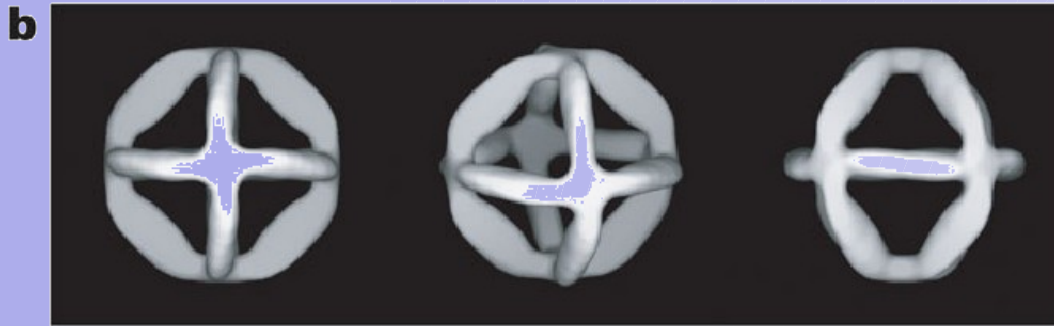
C Disabled T4 fuel-grabbing 'c'



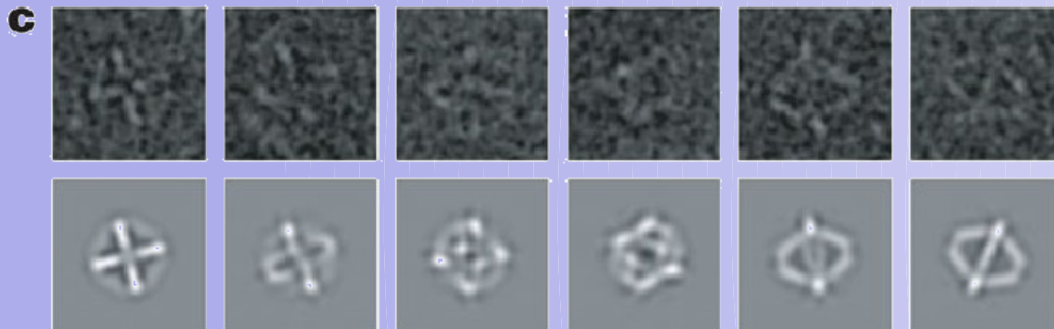
D Restored T4 fuel-grabbing 'c'



NANOSCALE OCTAHEDRONS (2)



b, Three views of the three-dimensional map generated from single-particle reconstruction of the DNA octahedron. c, Raw images of individual particles and corresponding map projections of the three-dimensional map.



The heavy-chain DNA can be amplified in the context of a bacterial plasmid and later excised, allowing its clonal production.